# Prediction of removal of Per- and Poly-fluoroalkyl Substances (PFAS) from drinking water by nanofiltration and reverse osmosis membranes

Analysing membrane flux variation over time and their ion removal efficiency

**WATER AND ENVIRONMENTAL ENGINEERING**
**DEPARTMENT OF PROCESS AND LIFE SCIENCE ENGINEERING | LUND UNIVERSITY**
**SUNEETA KAKATI | MASTER THESIS 2024**

# Prediction of removal of Per- and Poly-fluoroalkyl Substances (PFAS) from drinking water by nanofiltration and reverse osmosis membranes

Analysing membrane flux variation over time and their ion removal efficiency

by

## Suneeta Kakati

Master Thesis number: 2024-06

Water and Environmental Engineering
Division of Chemical Engineering
Lund University

June 2024

Supervisor: **Frank Lipnizki**
Co-supervisor: **Tobias Hey**
Examiner: **Åsa Davidsson**

# Preface

I would like to express my deepest gratitude to my supervisor, Frank Lipnizki, for his invaluable guidance and support throughout this research. Special thanks to my co-supervisor, Tobias Hey, for his continuous support and insightful suggestions during every stage of this project. Tobias's expertise and willingness to help have greatly enriched my research. I am immensely grateful for both his technical advice and moral advice.

I am also grateful to Per Falås for his guidance, which led me to Sofia Mebrahtu Wisén, who I thank for carrying out the water quality analysis in such a short time. I extend my heartfelt thanks to Mikael Sjölin for allowing me to use his automatic flux reading device, which significantly aided in my research. Lastly, I would like to thank my examiner, Åsa Davidsson, for helping me navigate through the challenges.

Many thanks to my mother for her support and encouragement. Her constant presence and belief in me have been a source of strength and motivation throughout this journey.

Finally, I extend my sincere gratitude to all the individuals who contributed to this study in various ways. Your support and assistance have been invaluable, and I am deeply appreciative of your contributions.

# Summary

Per- and polyfluoroalkyl substances (PFAS) are persistent environmental contaminants with significant health risks due to their resistance to natural degradation and potential adverse effects on human health. This study aims to evaluate the effectiveness of 8 commercial nano-filtration (NF) and reverse osmosis (RO) membranes in treating PFAS-contaminated drinking water. The objective was to assess the removal efficiency of total organic carbon (TOC), and various ions using a lab-scale membrane unit and thereby predict the PFAS removal of the membranes. The membranes were evaluated for their performance in terms of flux rates, ion rejections, and PFAS removal rate. The water quality was analysed before and after treatment to determine the efficiency of each membrane. Key operational parameters, such as trans-membrane pressure and crossflow velocity, and their impacts on membrane flux, fouling, and cleaning efficiency were also examined. The study observed that the NF membranes exhibited increased flux over time, whereas the RO membranes experienced a significant decrease in flux, however, ion removal efficiency was greater for the RO membranes, owing to their denser structure. Lastly, PFAS rejection rates of these membranes were predicted based on previous studies. In summary, NF and RO membranes were both effective in removing PFAS from drinking water, but each had specific operational and cleaning considerations. Future research should focus on addressing membrane fouling, optimising operational conditions, and integrating advanced treatment technologies to enhance PFAS removal efficiency for full-scale water treatment applications.

# Popular Scientific Summary

There are some harmful chemicals in the environment that pose significant health risks. These chemicals are called PFAS. Like many things, PFAS can end up in water and if that water is used as a drinking water source, PFAS can enter the human body and cause potential health issues including cancer and other chronic diseases. Therefore, it is important to ensure the safety of drinking water. To do this, water needs to be treated before using it for drinking purposes. Besides PFAS, there can be other harmful substances and minerals in the water that make it unsafe to drink. One way to treat water is through filtration, which helps separate the dirt or contaminants from the water.

Filtration can be considered as a filter paper that is used to make coffee, which separates the coffee grounds from the water. In water filtration, the water passes through membranes (similar to filter paper) that hold back the contaminants or dirt present/mixed in the water. There are different types of filter papers (membranes), and this study evaluated eight different water filter papers, known as nanofiltration (NF) and reverse osmosis (RO), to see how well they can remove the other contaminants from drinking water and thereby predict their effectiveness in removing PFAS.

Using a laboratory setup, the membranes were tested to measure their performance in terms of water flow and their ability to separate contaminants. The water quality was tested before and after filtration to determine how effective the filtration process was with the two different types of filter papers (membrane) used. It was found that NF membranes allowed more water to flow through over time because they have larger openings, similar to a coffee filter with bigger holes. The opposite was seen in the case of RO membranes because they have tighter openings, like a coffee filter with smaller holes. Because RO membranes have smaller openings, they were better at stopping contaminants from passing through, making the treated water much cleaner than water treated with NF membranes. However, one of the NF membranes also performed well at removing contaminants. As both NF and RO membranes were able to remove many contaminants, they are expected to be good at removing PFAS as well.

However, one limitation is that these membranes can get clogged over time. This is like filter paper getting dirty and jammed, making it harder for water to pass through. RO membranes usually have more of this problem because their openings are smaller, but this clogging behavior was not evident in this study. Membranes have another limitation; again, considering coffee filters, once coffee is ready, the coffee grains left on the paper are thrown afterwards in the waste, they cannot be broken down into smaller particles. Similarly, membrane filtration cannot break down the contaminants present in water and are released as waste which eventually end up in the environment.

Therefore, future research should focus on finding ways to minimize clogging and integrating new technologies with NF and RO membranes to break down these contaminants and make the treatment technologies even more effective.

# Table of Contents

# 1 Introduction

Per- and polyfluoroalkyl substances (PFAS) are anthropogenic chemicals formed by replacing hydrogen atoms with fluorine atoms in hydrocarbons. They were invented in the 1930s by the company DuPont, where an employee named Roy J. Plunkett accidentally created polytetrafluoroethylene (PTFE) (Blake and Fenton, 2020). PFAS are highly soluble in water, making drinking water a significant source of exposure (Emmett et al., 2006). Over 20 million people in Europe have been exposed to high levels of PFAS through drinking water (KEMI, 2023), and in Sweden, local exposure is higher in places with contaminated drinking water (KEMI, 2023). Several water sources in Sweden, including groundwater in Uppsala, are contaminated with PFAS (Sörengård et al., 2022).

PFAS are called forever chemicals due to their strong carbon-fluorine (C-F) bonds, which make them resistant to natural degradation and persistent in the environment (NIEHS, 2023). Some PFAS degrade very slowly, while others do not degrade at all. Polyfluorinated carbon chains are partially fluorinated, whereas perfluorinated carbon chains are fully fluorinated (Figure 1.1) (KEMI, 2023). Some PFAS are ubiquitous, persistent, toxic, and bioaccumulative, leading to their classification as persistent organic pollutants (POPs) under the Stockholm Convention (Jin et al., 2021).
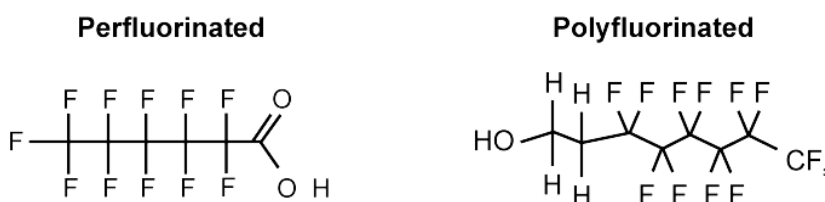


*Figure 1.1. Structure of Perfluorinated and Polyfluorinated Substances (KEMI, 2023)*

PFAS have diverse qualities and therefore widely used in various industrial and consumer applications, such as manufacturing cosmetics, non-stick cookware, lubricants, electronics, household items, firefighting foams, and paints (KEMI, 2023; Svenskt Vatten, 2022). Firefighting foams, in particular, are a significant source of drinking water contamination because of their excellent fire-resisting properties (OECD, 2013). Aqueous film-forming foams (AFFF), alcohol-resistant aqueous film-forming foams (AR-AFFF), and fluoro protein foams (FP) are commonly used in military, aircraft rescue firefighting (ARFF), municipal firefighting departments, petrochemical applications, and oil platforms (OECD, 2013).

Exposure to PFAS have raised concerns due to their potential health effects, including hormone imbalances, liver dysfunction, compromised immune systems, cancer, fertility disorders, and developmental impacts on young children (Johnson et al., 2019). PFAS commonly enter the environment through wastewater effluents from industries and municipalities manufacturing PFAS-related products (Das and Ronen, 2022). Conventional drinking water treatment plants, which include sedimentation, coagulation, flocculation, filtration, and disinfection units, are ineffective at degrading PFAS (Shivakoti et al., 2010). Thus, effective treat-

ment strategies are necessary to prevent PFAS from entering drinking water sources. Technologies such as adsorption and ion exchange resins have shown significant results in PFAS removal from drinking water (Hopkins et al., 2018). However, for short-chain PFAS, the adsorption capacity of conventional methods decreases, and the cost of regenerating or reactivating adsorbents like activated carbon can be very high (Liu et al., 2022). Additionally, higher concentrations of natural organic matter (NOM) or other contaminants can impact the PFAS rejection rate (Liu et al., 2022).

As longer-chain PFAS (i.e., $> C6$) are well-studied and known for their potential health threats, several government agencies have restricted their production or use (Peritore et al., 2023). However, the impacts of some short-chain PFAS are still undiscovered (European Commission, 2023). Due to their high stability, traditional treatments such as high-energy incineration are used to eliminate PFAS (Das and Ronen, 2022). These techniques are energy-intensive and costly, especially for large volumes of water. Consequently, membrane-based treatment processes like reverse osmosis (RO), nanofiltration (NF), and ultrafiltration (UF) have become increasingly popular for removing low concentrations of PFAS cost-effectively, with rejections as high as $> 99\%$ (RO) and 90-99% (NF) (Tang et al., 2007).

## 1.1 Aim

The study involved examining the variation of membrane flux of several commercially available NF and RO membranes over time, analyzing the removal of monovalent and divalent ions present in PFAS-contaminated drinking water, and assessing the suitability of these membranes in maintaining drinking water standards. This was conducted in a Lab-stack system operating at up to 50-75% water recovery. Additionally, the study sought to predict PFAS removal from drinking water by the studied NF and RO membranes. Drinking water from Sydvatten, pre-treated with biofiltration, was used. Membrane filtration was conducted, and samples were collected and sent for PFAS evaluation. Parameters such as electroconductivity, permeability, flow rate, pH, temperature, and pressure were focused on for the performance evaluation of the membranes.

## 1.2 Limitations

Due to an unexpected delay in the delivery of the lab-scale membrane unit, the final PFAS evaluation results were not completed within the scope of this report, as it is a time-consuming process. Consequently, this report includes a detailed discussion on the behavior of NF and RO membranes and a section on water analysis but lacks the final PFAS evaluation data. Time restrictions also prevented the examination of the long-term performance of the membranes. Moreover, while membrane filtration can separate PFAS, it cannot eradicate it entirely. If the concentrated membrane retentate is released without appropriate treatment, there is a risk of contaminating other water sources in the environment. The report does not address potential integration of membrane filtration with treatment methods like electrochemical oxidation or photocatalysis due to scope constraints.

## 1.3 Scope of this study

This study explains the treatment process of drinking water by using several commercial NF and RO membranes. Further examination is required to confirm the practicality of the membranes based on the recovery rate and to address challenges such as membrane fouling. While this study did not assess long-term membrane performance, it emphasizes the importance of evaluating efficiency and cost-effectiveness for real-world applications. Additionally, the re-

port highlights the need for further research on sustainable treatment solutions for PFAS-contaminated water.

# 2 Background

PFAS (Per- and Polyfluoroalkyl Substances) are naturally hydrophobic and oleophobic, showing great chemical and mechanical stability (Glüge et al., 2020). Over 4,700 species of PFAS have been detected in the environment (Pilli et al., 2021), with potentially many more yet to be discovered. Figure 2.1 provides an overview of different PFAS classes. Two of the most well-known subgroups of PFAS for their adverse health effects are perfluoroalkane sulfonic acids (PFSA), such as perfluorooctane sulfonate (PFOS), and perfluoroalkyl carboxylic acids (PFCA), such as perfluorooctanoic acid (PFOA) (KEMI, 2023). According to the US EPA, these compounds have estimated half-lives of over 41 and 92 years, respectively (Hara-Yamamura et al., 2022).
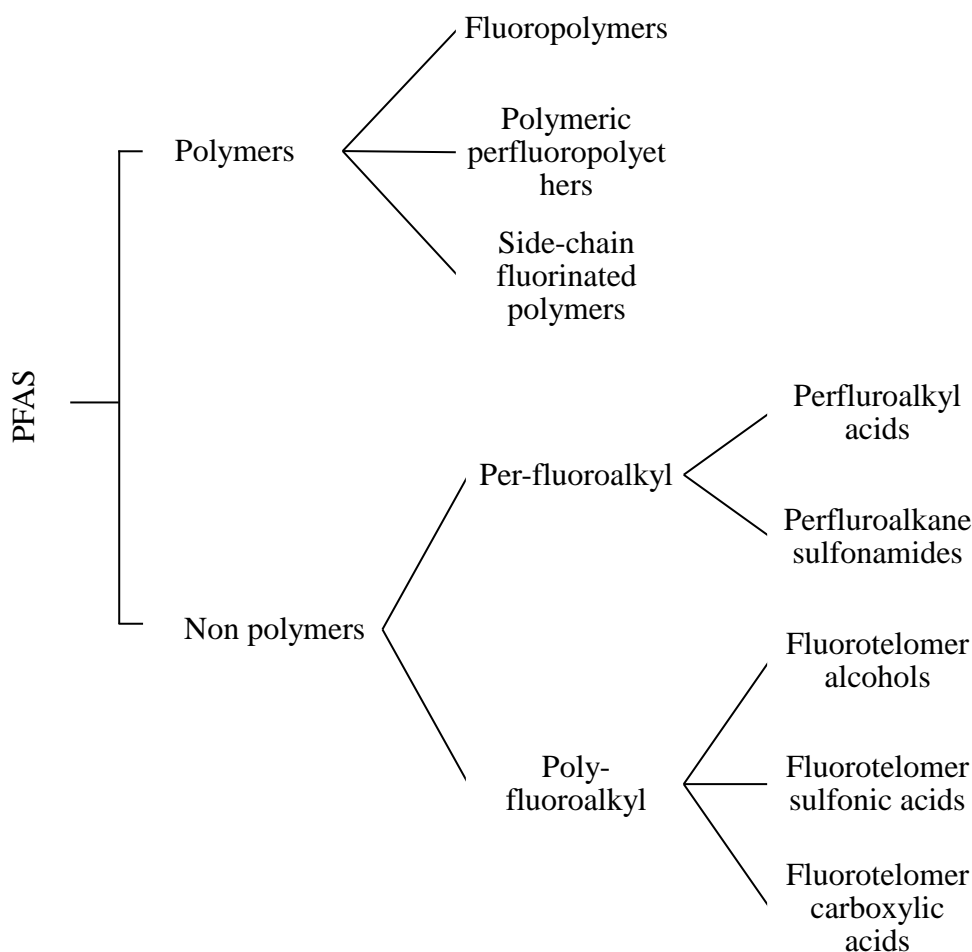


*Figure 2.1. General classification of per- and poly-fluoroalkyl substances (PFAS)(OECD, 2013)*

Low concentrations of PFAS have been detected in various aquatic environments, including lakes, rivers, and groundwater, as well as in fish, vegetables, and other foods grown in contaminated water and soil (Jin, Peydayesh, and Mezzenga, 2021). PFAS have also been found in human bodies, such as in contaminated blood, breast milk, and umbilical cord blood (Müller et al., 2019). Despite several guidelines aimed at restricting the production of these harmful substances, PFAS are still pervasive in the air, water, plants, and human bodies, essentially everywhere in the environment. Even if production ceases, their spread may continue indefinitely.

As mentioned in the introduction section PFAS have several health risks and these risks have led to the introduction of PFAS regulation and routine monitoring by the EU Drinking Water Directives, which set maximum limits on the total sum of individual PFAS concentrations and the sum of 20 specific PFAS, including carboxylates and sulfonates (EEA, 2024). The United States Environmental Protection Agency (U.S. EPA) and the World Health Organisation (WHO) have also set maximum limits for PFAS in drinking water. Various countries, such as the UK, Germany, Italy, the Netherlands, and Sweden, have developed individual guidelines and regulations to manage PFAS levels in drinking water, as shown in Table 2.1. Over time, these limits have become stricter in many organizations and countries.

*Table 2.1. PFAS limit for drinking water decided by different countries and organisations*

| Country/ Organisation | PFOA or PFOS (ng/L) | PFAS∑20 (ng/L) | PFAS∑4 (ng/L) | Total PFAS (ng/L) | Reference |
|---|---|---|---|---|---|
| **WHO** | 100 | ____ | ____ | 500 | Southerland and Birnbaum, 2023 |
| **U.S. EPA** | 4 | ____ | ____ | ____ | Furlow, 2024 |
| **EU DWD** | ____ | 100 | ____ | 500 | *EEA*, 2024 |
| **Denmark** | ____ | ____ | 2 | ____ | Southerland and Birnbaum, 2023 |
| **Germany** | ____ | 100 | 20 | ____ | Ingold, Kämpfe and Ruhl, 2023 |
| **Italy** | 30-500 | ____ | ____ | 500 | Giglioli, Colombo and Azzellino, 2023 |
| **Japan** | ____ | ____ | ____ | 50 | Hara-Yamamura *et al.*, 2022 |
| **Sweden** | ____ | 100 | 4 | ____ | *LIFE SOuRCE*, 2023) |
| **The Netherlands** | 200-390 | ____ | ____ | ____ | Kurwadkar *et al.*, 2022 |

## 2.1 Worldwide contamination of drinking water with PFAS

The persistence and widespread distribution of PFAS have resulted in significant contamination of drinking water sources globally. This section outlines the global prevalence and variation in PFAS contamination in drinking water, emphasizing the widespread and persistent nature of PFAS pollution across different regions and sources. Across continents and water systems, PFAS contamination has been detected, indicating the global reach of this issue. Despite geographical diversity, the consistent presence of PFAS highlights the need for comprehensive strategies to address this pervasive pollution. From industrialized nations to remote regions, the ubiquity of PFAS in drinking water underscores the urgent necessity for coordinated international efforts to mitigate its impact and safeguard public health.

Currently, around half of the human population relies on groundwater as their primary source of water. Unfortunately, these groundwater sources are often contaminated with various PFAS substances. For instance, Mojiri et al. (2023) reported PFAS levels as high as 51,000 ng/L in Swedish groundwater. Similarly, in China, PFAS levels in groundwater range from 5.3 to 615 ng/L in certain areas (Qiao et al., 2020), demonstrating the global nature of this contamination problem.

In addition to groundwater, many countries depend on surface water sources such as lakes, rivers, and reservoirs for their drinking water, which are also contaminated with PFAS. For example, high concentrations of PFAS have been detected in rivers that supply drinking water in countries like South Korea, Japan, Australia, and Ireland (Park et al., 2018). In South Korea, PFAS levels ranged from 1.44 to 224 ng/L, with compounds such as perfluorohexane sulfonate (PFHxS), perfluoropentanoic acid (PFPeA), perfluorohexanoic acid (PFHxA), and perfluorooctanoic acid (PFOA) being predominant.

In the United States, Crone et al. (2019) found PFOA and PFOS in both groundwater and surface water, with levels ranging from 10 to 2,305 ng/L and <5 to 821 ng/L, respectively. Seasonal variations also impact PFAS concentrations. Tokranov et al. (2021) discovered that PFAS concentrations were higher during winter at the interface between groundwater and surface water in Massachusetts. Major metropolitan regions in the U.S., such as Miami, Philadelphia, New Orleans, and the New York City suburbs, exhibit some of the highest levels of PFAS contamination. However, the U.S. EPA has not publicly disclosed specific contamination levels (Stoiber et al., 2020). PFBA and GenX were detected near industrial sources in North Carolina, Cincinnati, Ohio, Louisville, Kentucky, and New Orleans, Louisiana (Stoiber et al., 2020; Sun et al., 2016).

In Europe, over 20 million people have been exposed to high levels of PFAS (>100 ng/L for PFAS∑20) via drinking water (KEMI, 2023). Despite the American company 3M ceasing the manufacture of PFOA and PFOS in Belgium, PFOS concentrations remain high near the chemical plant in Antwerp (ZeroWater Europe, 2022). Similarly, Dupont or Chemours contaminated air and water consumed by 750,000 people in Dordrecht, Netherlands, with PFOA and GenX (Heal, 2018). In the Veneto region of Italy, the chemical plant Miteni contaminated drinking water with PFOA, affecting over 350,000 people (CHEM Trust, 2023). In 2013, PFOA and PFOS levels in drinking water were found to be 1,475 ng/L and 117 ng/L, respectively, exceeding Italian government limits (Manea et al., 2020). A study in Barcelona, Spain, revealed that the most prevalent PFAS compounds in drinking water were PFPeA, PFBS, PFHpA, PFHxA, and PFOS (Cserbik et al., 2023). Seasonal variations in PFAS concentrations were observed in the Ter and Llobregat river waters. PFPeA and PFBS were the most

detected substances during one sampling period, with concentrations of 4 ng/L and 6.8 ng/L, respectively.

The Nordic Council of Ministers studied PFAS presence in Denmark, Finland, Greenland, Iceland, Norway, Sweden, and the Faroe Islands in 2017 (Kärrman et al., 2019). In Denmark, firefighting foams were a major source of contamination (Heal, 2018). In Sweden, various activities by the Swedish Armed Forces contributed to contamination in places like Botkyrka, Båstad, Halmstad, Uppsala, Ängelholm, Östersund, and Ronneby (Svenskt Vatten, 2022). For example, in Ronneby, 165 municipality members were exposed to high levels of PFAS due to contaminated drinking water (Svenskt Vatten, 2022). Similarly, in Uppsala, the groundwater reservoir was heavily contaminated by PFAS due to military activities at Ärna Airport (Glynn, 2012; Gyllenhammar et al., 2015). Gyllenhammar and Bergström (2014) concluded that the main cause of PFAS contamination in Sweden was the use of AFFF containing PFAS at military airports between 1985 and 2003. Nguyen et al. (2022) found that firefighting foams significantly impacted PFAS levels in a river catchment in Sweden.

To further illustrate the extent of PFAS contamination in drinking water worldwide, Table 2.2 presents maximum PFAS concentration levels from various countries across different continents. This data, sourced from studies referenced in the table, emphasizes the global prevalence of PFAS pollution. Additionally, a visual comparison of these concentrations is provided through a map (see Figure 2.2.) generated using QGIS (Quantum Geographic Information System), enhancing our understanding of PFAS contamination on a global scale.

*Table 2.2. Maximum PAFS concentration levels found the mentioned literature studies in drinking water in different countries*

| Country Name | Continent | PFAS (ng/L) | Reference |
|---|---|---|---|
| **Australia** | Oceania | 16 | Thompson, Eaglesham and Mueller, 2011 |
| **China** | Asia | 502 | L. Liu *et al.*, 2021 |
| **Germany** | Europe | 519 | Domingo and Nadal, 2019 |
| **Hong Kong** | Asia | 39 | Li *et al.*, 2021 |
| **Ireland** | Europe | 1.7 | Harrad *et al.*, 2019 |
| **South Korea** | Asia | 644 | Kim *et al.*, 2020 |
| **Sweden** | Europe | 25 | Woldegiorgis *et al.*, 2005 |
| **Taiwan** | Asia | 20 | Jiang *et al.*, 2021 |
| **Uganda** | Africa | 5.3 | Arinaitwe *et al.*, 2021 |
| **U.S.A** | North America | 213 | Skaggs and Logue, 2021 |
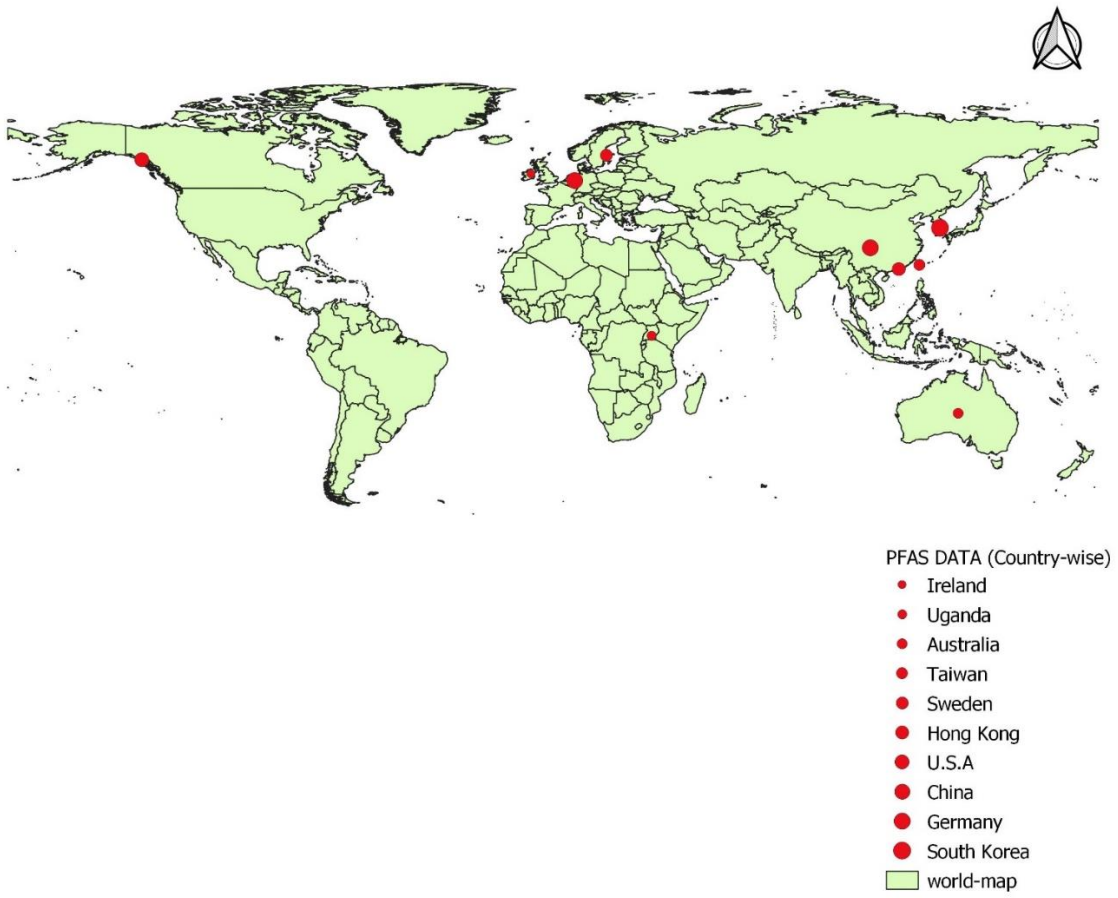
*Figure 2.2. Map of drinking water PFAS concentration in the countries mentioned in Table 2.1. using QGIS*

## 2.2 Sources of PFAS in drinking water, country-wise

The sources of PFAS contamination vary from country to country. PFAS are spread through various types of routes, including industries, landfills, military bases, and more. This section consists of the sources of PFAS contaminating the drinking water in several parts of the world (Table 2.3).

*Table 2.3. PAFS sources causing drinking water contamination for different countries*

| Country | Main Contamination Source | Reference |
|---|---|---|
| **South Korea** | Industries | Park *et al.*, 2018 |
| **China** | Landfills | Yan *et al.*, 2015 |
| **Spain** | Industries | Flores *et al.*, 2013 |
| **Japan** | Military bases | Metcalfe *et al.*, 2022 |
| **Italy** | Industries | *Regione del Veneto, Patrocinio & WHO*, 2017 |
| **Sweden** | Swedish Armed forces | *Svenskt Vatten*, 2022 |

The evidence of the presence of PFAS in drinking water sources has increased the requirement of finding suitable methods for their removal, taking into account the consequences, such as waste generation and maintenance of the concentrated residuals etc. Depending on the water type, the PFAS remediation methods and their effects could vary since the type and concentration could be different in different water types. Traditional treatments techniques like advanced oxidation and incineration are energy-intensive and costly (Das and Ronen, 2022). Membrane filtration is known for its ability to remove emerging micropollutants such as pesticides, pharmaceuticals, endocrine-disrupting compounds, and also PFAS from natural waters (Liu *et al.*, 2022). Using dense membranes like nanofiltration (NF) and reverse osmosis (RO) membranes, is an efficient and sustainable way for removing PFAS from water. Several studies have shown that NF and RO can remove a wide variety of PFAS with efficient removal rates (RO>99%, NF = 90%-99%) (Liu, Strathmann and Bellona, 2021; (Liu *et al.*, 2022; Mastropietro *et al.*, 2021; Tang *et al.*, 2007). RO membranes have a denser active layer than NF and are widely employed for PFAS removal in commercial and industrial applications.

## 2.3 Characteristics of NF and RO membranes

For PFAS treatment, organic (polymeric) NF membranes are generally more advantageous than inorganic membranes due to their low cost, easier processing, and robustness (Jin et al., 2021). Commercial NF and RO membranes are predominantly thin film composite (TFC) polyamide (PA) membranes. TFC membranes typically consist of three layers, i.e. on top there is a thin selective fully aromatic or semi-aromatic piperazine-based PA layer, a nanoporous polysulfone support layer, and lastly, a non-woven fabric layer for mechanical stability (Zhu et al., 2021). In practice, the membrane properties and performances of NF and RO are primarily determined by the top layer, recognised as the active separation layer (Petersen, 1993). Both NF and RO have low molecular weight cut-offs (MWCOs), with RO having the lower, in the range of ≤ 100 Da and ~ 0.1 nm, whereas for NF membranes, the range is between 90 and 1000 Da (0.3–2.1 nm) (Liu, Strathmann and Bellona, 2021). Although RO membranes have higher rejection than NF and is capable of removing most types of organic and inorganic contaminants from water, RO-treated water is not directly suitable for drinking purposes. That is why, a post-treatment process is mostly carried out after the RO treatment to ensure the alignment of the water quality with the drinking water standards (Bolisetty, Peydayesh and Mezzenga, 2019). The removal rate of PFAS can vary depending on their chain length. Long-chain PFAS, such as PFOS, are always easier to remove than short-chain ones since PFOS have a molecular weight high enough to be restrained by NF or RO membranes. In a study by Appleman *et al.*, (2013), rejection rates for 9 perfluoroalkyl acids (PFAAs) were over 93%, along with a trend towards higher rejection rates for PFAAs with higher molecular weights. Typically, the rejection rates of long-chain PFAS by NF membranes ranges between 85%-95%, whereas they decrease to 20-70% for short-chain ones (Jin et al., 2021). However, RO has usually better rejections, due to its dense active layer of rejection. Jin, Peydayesh and Mezzenga, 2021 have reported in their review that more than 71% of PFOA and PFOS rejection rates could be achieved by using a wide range of nanofiltration membranes (both commercial and prepared) spanning MWCO from 100 to 900 Da. On the other hand, the reverse osmosis (RO) process showed a complete removal for both PFOA and PFOS since RO can restrain more substances due to having membrane pore sizes lower than NF membranes. Short-chain PFAS are always difficult to remove, however, it has been observed that RO could remove some of the short-chain PFAS as well (Jin et al., 2021). Nevertheless, permeate flux decreases with decreasing membrane pore sizes (Zouhri et al., 2017), whereas the removal of total organic carbon (TOC) increases with decreasing membrane pore size. For instance, Bates et al., (2021) recorded a rejection of >95% and >99% TOC by NF and RO membranes, respectively. Moreover, feed water composition plays an important role in the membrane's overall performance, such as pH, operation conditions and the presence of organic matter and inorganic ions are some important factors which can alter the PFAS removal efficiency of the membranes.

## 2.4 Factors affecting PFAS removal by NF and RO

### 2.4.1 Operational conditions (TMP, CP and Temperature)

Depending on the operational conditions, the removal rate of PFAS from the contaminated water could vary, among which transmembrane pressure (TMP), temperature, and feed concentration. NF and RO membranes are pressure driven so their performance heavily depends on TMP, and TMP and membrane flux are directly proportional to each other and so the salt rejection and TMP (Jin et al., 2021). Therefore, the flow of permeate will increase as TMP increases and the contaminant concentration will decrease in the permeate. Moreover, Concentration Polarization (CP) occurs when solutes accumulate near the membrane surface, which can in turn increase membrane fouling (Jin et al., 2021). Nevertheless, Jin(2021), mentioned that increase in TMP and so the flux will help decrease the growth of these solutes. Higher CP, however, can reduce both water flux and rejection rates (Soriano, Schaefer and Urtiaga, 2020). Another important factor to be considered is the operating temperature. Membrane pore size increases with an increase in temperature due to thermal expansion and so the solute movement through the membrane, since their viscosity decreases with increase in temperature (Jin et al., 2021).

### 2.4.2 Effect of contaminants concentration

The initial concentration of PFAS in the feed affects permeate flux and removal efficiency. Normally, solutions with higher PFAS concentrations are more complicated than diluted PFAS solutions. High concentrations may lead to micelle formation, if the initial PFAS concentration in the water crosses the critical micelle concentration (CMC), influencing removal outcomes (Jin et al., 2021). As PFAS concentrations rise to the CMC and aggregate into micelle forms, Concentration Polarization (CP) film degrades which increases permeate flux close to that of pure water levels (Hang *et al.*, 2015). Hang *et al.*, (2015), further mentioned that the PFAS rejection rate increases due to the decrease in CP. Based on studies by Wang *et al.*, (2018), increasing concentrations of both PFOS and PFBS led to improved PFOS and PFBS adsorption on the membrane surface, and increased rejection rates, respectively from 88.3% to 92.5% for PFOS and 47.7% to 50.4% for PFBS. Additionally, higher initial PFAS concentration can lead to lower the membrane flux (Tang *et al.*, 2006).

### 2.4.3 Effect of Membrane Surface Properties

Organic NF membranes, with their negative charge and hydrophilicity, demonstrate advantages in PFAS removal—the active layer's characteristics, such as low molecular weight cutoff, impact membrane performance (Das and Ronen, 2022). Concentration polarization and micelle formation on the membrane surface can affect PFAS rejection. In addition to the active layer properties, membrane pore size and porosity play a critical role in PFAS rejection; membranes with tight and dense structures have higher PFAS removal than loose-structured ones (Zhi *et al.*, 2022). The rejection of PFAS decreases as MWCO increases, and the predominant mechanism of PFAS removal by NF membranes is steric hindrance mediated by molecular size-pore size interactions (Zhi *et al.*, 2022). Moreover, the relation between water permeability, salt selectivity, and PFAS rejection is also important to take into account.

### 2.4.4 Effect of pH and membrane materials

One of the important feedwater parameters, pH, has a crucial impact on the membrane surface charge and so on the pores. The removal rate increases with increasing pH. On the other hand, when the feedwater has a low pH, it can reduce the pore sizes of the membrane by minimizing the electrostatic repulsion inside the pores, in that case, removal occurs mainly through steric

exclusion (Liu *et al.*, 2022). When the initial pH is more basic, the removal rate is faster. Zeng et al., (2017) showed that the PFHxA rejection rate was enhanced due to the reduction of membrane pore size because of low pH levels. However, in the case of RO membranes, Soriano, Gorri and Urtiaga, 2019 have noticed a higher PFHxA removal at the neutral pH with a more negatively charged membrane surface.

### 2.4.5 Effect of ions and ionic strength

When anions have a higher valence, electrostatic interaction increases, and the removal rate is directly proportional to electrostatic interaction (Das and Ronen, 2022). Even though cations have comparatively less effect on PFAS removal and reduce the rejection by minimizing electrostatic interactions between solutes and membranes, $Ca^{2+}$, $Mg^{2+}$ ions can agglomerate with PFAS molecules and therefore enhance the removal by increasing their molecular weight (Zhao *et al.*, 2013, 2016). In addition, $Ca^{2+}$, $Pb^{2+}$, and $Fe^{3+}$, such multivalent metal ions can block the membrane pores by forming bridges between the PFAS molecules and increasing the PFOS rejection rate (Luo et al., 2016) and (Zhao et al., 2017). The removal rate of PFAS from NF membranes can be influenced by ionic strength differently depending on the removal mechanism. In the case of size exclusion, Wang *et al.*, (2018) reported an increase in removal rate with increasing ionic strength; however, the removal rate decreases with electrostatic repulsion. Due to having negatively charged surface, NF membranes decrease in surface charge with increasing ionic strength, which decreases electrostatic repulsive forces between the membrane surface and target molecules, resulting in lower removal rates (Wang *et al.*, 2018). With increasing ionic strength, Wang *et al.*, (2018) further reported that PFBS rejection decreased to 20.5%; meanwhile, PFOS rejection increased from 89.6% to 91.9%, indicating different predominant removal mechanisms for the NF membranes for both PFASs. Moreover, PFAS chain length and their interaction with electrostatic forces have a significant role in the removal rate.

### 2.4.6 Effect of organic matter

The presence of a higher concentration of natural organic matter (NOM) in the water can cause fouling on the surface of the membrane. Due to their nature, NOM can bind with other pollutants present in the water and make a gel layer on the membrane surface (Jin et al., 2021), resulting in an increasing rejection rate. Based on Zhao et al., (2016) results, humic acid (HA) slightly improved PFOS removal efficiency from 94.1% to 95.1%. However, a remarkable reduction of permeate flux has been observed due to fouling. On the contrary, the rejection rate could also decrease if there are divalent cations, such as $Ca^{2+}$ is present (Das and Ronen, 2022). When NOM interacts with these ions and deposits on the membrane surface, it affects the electrostatic interactions negatively, as a result, the PFAS rejection rate decreases (Das and Ronen, 2022). Das and Ronen, 2022 further mentioned that PFAS rejection is substantially reduced by these ions and organic matter due to fouling-enhanced concentration polarization, which results in greater solute concentrations at the membrane surface.

## 2.5 Mechanisms of PFAS removal by NF and RO membranes

Jin, Peydayesh and Mezzenga, 2021 have stated that steric (size) exclusion, solution-diffusion, and electrostatic interaction are the main mechanisms governing PFAS rejection by NF and RO membranes. In the case of the steric (size) exclusion mechanism, the removal is mainly dependent on the membrane's molecular weight cut-off (MWCO). A membrane with higher MWCO will show lower removal than one with lower MWCO. For example, Das and Ronen, 2022 mentioned that NF90 (DuPont) (MWCO 100-200 Da) led to a rejection of 99.8% of PFHxA, whereas, for NF270 (DuPont) (MWCO 300 Da), it was 96.2%. RO membranes excel in steric exclusion and achieve higher rejection rates due to a lower molecular weight cut-off (MWCO 100 Da) (Das and Ronen, 2022; Dagher *et al.*, 2023; Ma *et al.*, 2024). Ions like $Mg^{2+}$, $Ca^{2+}$, and $Fe^{3+}$ can form bridging structures, and form larger substances thereby enhancing PFAS retention during the NF process (Jin et al., 2021). Membrane surfaces are usually charged, for example, NF has a negatively charged surface. Electrostatic forces develop when the charged membrane surfaces interact with charged organic pollutants. These electrostatic forces play a significant role in membrane performance, and for short-chain PFAS, electrostatic repulsion is effective (Jin et al., 2021). It has been demonstrated that electrostatic interactions are affected by both ion strength and pH, as well as by the amount of dissociation of organic solutes at the membrane surface (Mo et al., 2008). When short-chain PFASs, like PFHxA, encounter membranes with similar or larger MWCO, electrostatic interaction dominates, whereas size exclusion is relatively weak (Zeng et al., 2017). Last but not least, in the solution-diffusion mechanism, rejection is determined by the different diffusivities and solubilities of the NF/RO membrane (Wijmans and Baker, 1995; PAUL, 2004). In this case, PFAS diffuses across the membrane as a result of their dissolution in the thin film of NF/RO. A set of commercial NF and RO membranes are listed in Table 2.3 including their characteristics and PFAS removal rates based on the previous studies.

*Table 2.3 NF and RO membrane types and their characteristics with previous PFAS rejection data*

| Membrane type (NF/RO) | Producer | Membrane Type | pH range | Max. Temperature | Max. Pressure | Salt Rejection | Test Condition | PFAS Rejection | Reference |
|---|---|---|---|---|---|---|---|---|---|
| **FilmTec™ NF90 (MWCO =90–200Da)** | DuPont | Polyamide Thin-Film Composite | 2.0-11.0 | 45°C | 41 bar | 97-98.7 % | 2,000 ppm MgSO4, 25°C and 15% recovery at 4.8 bar | 90-99% PFOS > 98.3% (PFAA - PFPeA, PFHxA. PFOA, PFPrS, PFBS, PFPeS, PFHxS, PFHpS, PFOS) | (Tang *et al.*, 2007) |
| **FilmTec™ NF200 (MWCO <300Da)** | DuPont | Polyamide Thin-Film Composite | ____ | ____ | 41 bar | ____ | Feedwater MgSO4 2,000 ppm, Pressure 4.8 bar, Temperature 25°C, pH 8, Recovery 15%, Test time 20 min | ≥ 95% PFAS, except 72% PFPnA | (Steinle-Darling and Reinhard, 2008) |
| **FilmTec™ NF270 (MWCO = 155–300Da)** | DuPont | Polyamide Thin-Film Composite | 3.0-10.0 | 45°C | 41 bar | >97 % | 2,000 ppm MgSO4, 25°C and 15% recovery | 90-90% PFOS<br><br>41.9 % (PFPrS) , PFPeA 76.8%, PFBS 55.4%, PFHpS 79.5%, 88.4 % (PFOA), PFOS 76.5%, PFHxS 79.5%, PFHxA 78%<br><br>≥ 95% PFAS (PFPeA, PFHxA, | (Tang *et al.*, 2007)<br><br>(Safulko *et al.*, 2023)<br><br>(C. J. Liu *et al.*, 2021) |

| | | | | | | | | PFHpA, PFOA, PFPeS, PFHxS, PFHpS, PFOS, FHxSA and 6:2 FTS), Expect PFSAs (PFBS and PFPrS) between 88 and 93% (at 90% recovery rate) | |
|---|---|---|---|---|---|---|---|---|---|
| **NF-DL (MWCO 150-300 Da)** | Veolia - Suez | Thin-Film Membrane | 2.0 – 11.0 | 50°C | 41 bar | MgSO4 96% | 2,000 ppm MgSO4 solution at 110 psi operating pressure, 25°C, 15% recovery | PFC >95% Except FOSA 42% | (Steinle-Darling and Reinhard, 2008) |
| **NF-DK (MWCO 150-300 Da)** | Veolia - Suez | Thin-Film Membrane | 2.0 – 11.0 | 50°C | 41 bar | MgSO4 98% | 2,000ppm MgSO4 solution at 110 psi operating pressure, 25°C, 15% recovery | PFOS (90-90%) | (Tang *et al.*, 2007) |
| **FilmTec™ BW30 (MWCO 98Da)** | DuPont | Polyamide Thin-Film Composite | 2.0-11.0 | 45°C | 41 bar | 98-99.5% | 2,000 ppm NaCl and 15.5 bar, pH 8, 25°C and 15% recovery | 99% PFOS | (Safulko *et al.*, 2023) |
| **FilmTec™ XLE (MWCO 100Da)** | DuPont | Polyamide Thin-Film Composite | 2.0-11.0 | 45°C | 41 bar | 97.0 - 99.0% | 2,000 ppm NaCl, 8.6 bar, 25°C, pH 8, 15% recovery | 99.7% PFHxA | (Soriano, Gorri and Urtiaga, 2019) |

## 2.6 Pre-treatment of feedwater

NF and RO have proven to be significantly effective in removing PFAS. However, premature membrane fouling is one of the primary limitations associated with NF and RO, which can result in other related problems. For instance, operating and maintenance cost increases due to the demand of higher operating pressure and frequent cleaning and their service life decreases as well (Ahmed, Amin and Mohamed, 2023). These limitations are both due to membrane characteristics and hydrodynamics within the membrane module (Liu *et al.*, 2022). Several problems related to NF and RO such as fouling, could be solved by using pre-treatment methods, for example, coagulation/flocculation, biofiltration and so on (Jin et al., 2021). At the same time, it might also require excessive pre-treatment units, material, energy, and chemicals thus increasing the overall capital investment and operating and maintenance costs (Liu *et al.*, 2022).

### 2.6.1 Coagulation and/or flocculation
The process of coagulation destabilizes the solution or suspension. A flocculation process, on the other hand, combines the destabilized particles and produces larger aggregates. Various coagulants can be used, including inorganic (e.g. alum, ferric chloride, and polyaluminium chloride) and organic (e.g. gelation and cetyltrimethylammonium bromide (CTAB)) (Jin et al., 2021). PFAS removal efficiency is primarily determined by coagulant adsorption ability, with long-chain PFAS being more effective than short-chain ones. As a result of coagulation and flocculation, the rejection rate is improved significantly along with the permeate flux (Jin et al., 2021). Yu et al., (2016) have reported that an increase from 55 to 86% of PFOS rejection was noticed by carrying out the coagulation before passing the water through NF.

### 2.6.2 Biofiltration
Biofiltration is the process of biological water treatment for reducing the organic components, e.g. Biological Oxygen Demand (BOD), Natural Organic Matter (NOM), that either cause organic fouling or provide carbon sources for biofilm growth on the surface of the membranes. Several processes are used in the biotreatment of drinking water, including granular active carbon (GAC) filters, rapid sand filters (RSFs), and slow sand filters (SSFs). Biological filtration is primarily used to remove biodegradable organic carbon (Hammes *et al.*, 2011). Two main steps are involved in a biofiltration process. The first step is passing pollutants upstream or downstream through the filter bed. After the first step, pollutants undergo biodegradation. In a biofilter, biofilm plays a key role in the treatment of pollutants, which can be formed from a variety of microbes, e.g. bacteria, yeasts, fungi, algae, and/or nematodes (Abubackar *et al.*, 2019). Hydraulic retention time (HRT) is considered the most important operational factor in biofiltration. It represents the food supply for the microorganisms present in the biofilm and also the total contact time of the microbes with pollutants in the water. Suprihatin et al., (2017) have observed organics, turbidity, TSS, ammonium ($NH_4$-N) and colour could be removed up to 77.7%, 84.1%, 91.1%, 81.9% and 86.1% respectively with an HRT of 2 hours. However, this study does not intend to focus on or provide a detailed explanation of the pretreatment of feedwater.

## 2.7 CIP / Chemicals concerning drinking water

Membrane fouling is a concern for performance longevity, occurs in most types of membranes after running for a certain period. Due to membrane fouling, the permeate flux decreases and the membrane is no longer useful to treat PFAS-contaminated water unless cleaned properly, ultimately adding to the total treatment costs. Therefore, chemical cleaning agents play a vital role in achieving a satisfactory removal rate while maintaining the permeate flux. Nevertheless, when applying for drinking water treatment, there are many restrictions on the usage of chemicals. Different countries have different regulations, for Sweden the maximum limit on the allowed cleaning chemicals is 5 mg/l (SLVFS, 2001).

# 3 Materials and Methods

## 3.1 Water collection

The water samples analyzed in this study were drawn from the tap water provided by Sydvatten drinking water supplier, serving approximately ca. 1 million residents in Skåne *(Vombverket, 2015)*. Sydvatten operates two drinking water treatment plants (DWTPs): Vombverket and Ringjöverket. Vombverket sources its raw water from Lake Vombsjön and employs a comprehensive purification process involving artificial infiltration, aeration, softening, chemical cleaning with ferric chloride, sand filtration, UV light treatment, and final chlorine disinfection *(Vombverket, 2015)*. Conversely, Ringsjöverket draws its raw water from Lake Bolmen and treats it through chemical precipitation, rapid and slow-sand filtration, UV light treatment, and chlorine disinfection *(Ringsjöverket, 2015)*. This study specifically focuses on water samples from Vombverket, which supplies Burlöv, Malmö, Staffanstorp, Svedala, Vellinge, and parts of Lund and Eslöv *(Vombverket, 2015)*.

## 3.2 PFAS spike solution

A standard PFAS spiking solution (FX19) was prepared in the laboratory of Swedish University of Agricultural Sciences (SLU) and sent to Lund University for performing the tests. This spike solution contains 15 PFAS compounds as listed in Table 3.1. The PFAS evaluated spanned a range of chain lengths (C3 – C13) and were composed of both perfluoroalkyl-carboxylic and -sulfonic acids. The stock solution contains a concentration of 0.10 mg/mL of each PFAS considered in this study.

*Table 3.1. PFAS and their MWCO (Ahrens et al., 2012; Kim et al., 2015; Wang et al., 2011)*

| PFAS Compound | Category | MW [g/mol] |
|---|---|---|
| **PFBA (C$_3$)** | Carboxylic, short-chain | 213.04 |
| **PFPA (C$_6$)** | ———— | 310.05 |
| **PFHxA (C$_5$)** | Carboxylic, short-chain | 314.1 |
| **PFHpA (C$_6$)** | Carboxylic, short-chain | 363.07 |
| **PFOA (C$_7$)** | Carboxylic, long-chain | 414.1 |
| **PFNA (C$_8$)** | Sulfonic, long-chain | 463.09 |
| **PFDA (C$_9$)** | Sulfonic, long-chain | 513.10 |
| **PFUnDA (C$_{10}$)** | Sulfonic, long-chain | 563.11 |
| **PFDoDA (C$_{11}$)** | Sulfonic, long-chain | 613.12 |
| **PFTeDA (C$_{13}$)** | Sulfonic, long-chain | 713.14 |
| **PFBS (C$_4$)** | Sulfonic, short-chain | 300.1 |
| **PFHxS (C$_6$)** | Sulfonic, short-chain | 400.1 |
| **PFOS (C$_8$)** | Sulfonic, long-chain | 500.1 |
| **FOSA (C$_8$)** | Sulfonic, long-chain | 499.18 |
| **6:2 FTSA (C$_8$)** | Sulfonic, long-chain | 428.17 |

## 3.3 Membranes

In total 8 flat-sheet polymeric commercial nanofiltration and reverse osmosis membranes were selected for the removal of PFAS from the collected drinking water samples. The membrane products selected included four NF membranes i.e. FilmTecTM NF90 (DuPont), FilmTecTM NF270 (DuPont), NF99HF (Alfa Laval) and NF (Alfa Laval), and four RO membranes namely, FilmTecTM BW30 (DuPont), Alfa Laval RO99, Alfa Laval RO98 pHtTM, and Alfa Laval RO90. NF and RO membranes were selected based on their characteristic separation performances. A summary of the properties and characteristics of the membranes evaluated during this study is shown in Table 3.2.

*Table 3.2. Summary of membrane characteristics tested at MemLab, Lund University*

| | Membrane | Manufacturer | Pressure (bar) | Temperature (°C) | pH |
|---|---|---|---|---|---|
| **NF Membranes** | **FilmTec™ NF90** | DuPont | 4.8 bar (typical) | 45 | 1 – 10.5 |
| | | | 41 bar (max.) | 35 (>pH 10) | |
| | **FilmTec™ NF270** | DuPont | 4.8 bar (typical) | 45 | 3 – 10 |
| | | | 41 bar (max.) | 35 (>pH 10) | |
| | **NF99HF** | Alfa Laval | 15 – 41 (typical) | 5 – 50 | 1.5 – 10 |
| | | | 55 (max.) | | |
| | **NF** | Alfa Laval | 15 – 41 (typical) | 5 – 50 | 1.5 – 10 |
| | | | 55 (max.) | | |
| **RO Membranes** | **FilmTec™ BW30** | DuPont | 4.8 bar (applied) | 45 | 1 – 10.5 |
| | | | 41 bar (max.) | | |
| | **RO99** | Alfa Laval | 14 – 41 (typical) | 5 – 50 | 1.5 – 11 |
| | | | 55 (max.) | | |
| | **RO98pHt™** | Alfa Laval | 14 – 41 (typical) | 5 – 60 | 1.5 – 12.5 |
| | | | 55 (max.) | | |
| | **RO90** | Alfa Laval | 14 – 41 (typical) | 5 – 50 | 1.5 – 11 |
| | | | 55 (max.) | | |

## 3.4 M20 Pilot system

A TestUnit M20 pilot system (Alfa Laval, Denmark) was used for membrane evaluation experiments (see Figure 3.1). The unit consists of a high-pressure pump, tank, heat exchanger, valve, pressure gauges, and hydraulic hand pump for module compression. With a membrane area ranging from 0.036 $m^2$ to 1.8 $m^2$, the system is flexible and allows the simultaneous testing of different membrane types. A maximum of 40 flat-sheet polymeric membranes, 20 support plates (Figure 3.2 (a)) and 21 spacer plates (Figure 3.3 (b)) can be tested at the same time with separate permeate-outlets from each membrane pair. The pilot system allows a cross-flow varying from 3.5 L/min to 24 L/min and can be used for multiple purposes by combining plate-and-frame and spiral wound designs in one unit. The feed tank has a total volume of 7.5 liters. The M20 TestUnit in operation during the Reverse osmosis (RO) membrane filtration is presented in Figure 3.3. The plate-and-frame unit has open channels that allow feed/retentate to flow across the membrane surface. With the permeate collecting tubes, the permeate from the membrane is collected and removed from the unit through hollow plates with numerous slots. Feed/retentate are sealed off by the membrane itself, assisted by lock rings or strips, to prevent mixing with permeate in plate-and-frame systems, which also protect the plate stack from leakage.
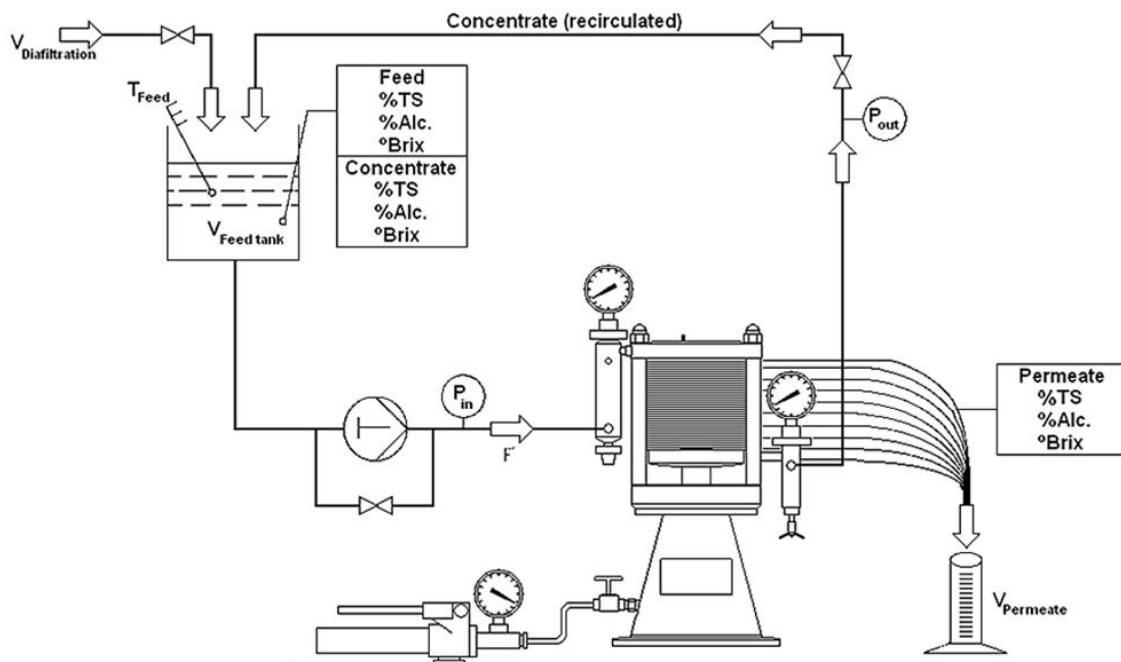


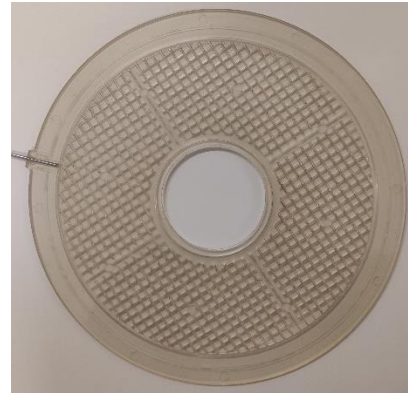*Figure 3.1. TestUnit M20 pilot system (Alfa Laval, Denmark)*

*Figure 3.2. a) Spacer plate, b) Support plate of M20 TestUnit*



*Figure 3.3. TestUnit M20 pilot system in performance during RO membrane filtration, Mem-Lab, Lund University*

## 3.5 Chemicals

The cleaning agent, Ultrasil 110, used for cleaning the membranes, was purchased from ECOLAB. Membranes were conditioned before use and cleaned before disposal using Ultrasil 110 (Figure 3.4). For quality assurance, to check the integrity of the membranes, Sodium Chloride (NaCl) and Magnesium Sulphate ($MgSO_4$) were used after the conditioning step. A detailed explanation is given in the following section.
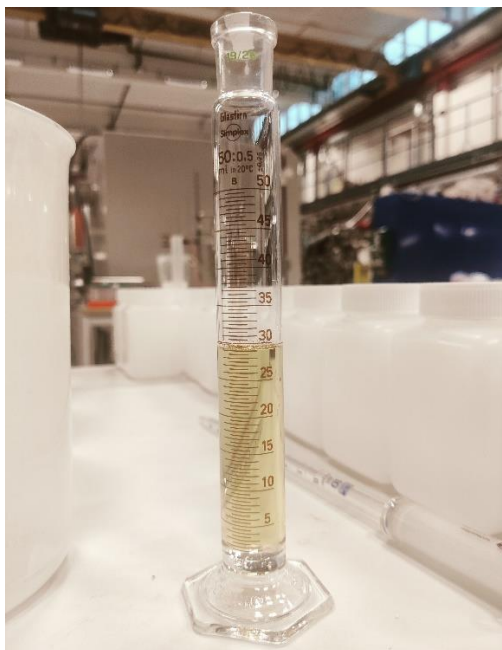


*Figure 3.4. 30mL of Ultrasil 110 (extra to cover up the vacuum) in a measuring cylinder during NF/RO membrane filtration, MemLab, Lund University*

## 3.6 PFAS rejection experiments including operating conditions

In the study, a total of six experiments were carried out to evaluate the performance of nano-filtration (NF) and reverse osmosis (RO) membranes. Initially, the setup required measuring the dead volume and recovery rate in the feed tank and preparing the membranes by cutting them to fit the M20 system. Total 3 group experiments, all NF membranes were tested together in one group, followed by all RO membranes (second group). A total of 4 types of NF and RO membranes (each) were used but due to the specific design of M20 system, 16 sheets of RO membranes were used and assembled them into the system as depicted in Figure 3.5. Also, Table 3.3 gives a clear about permeate number and their corresponding membrane type. To achieve an equal average pressure distribution, similar membrane types are placed one at the top and one at bottom. However, in the case of NF, due to the unavailability of sufficient number of NF (Alfa Laval) membrane type, the total number of membrane sheets used was 14, with NF (Alfa Laval) in the center (to maintain the average pressure distribution). Each group was subjected to three replicate experiments, however, the order is individual's choice, as long as the average pressure is distributed equally in all types of membranes used. The experimental setup involved stacking the membranes in pairs. As depicted in Figure 3.6 with

the membrane side facing outwards and paper side inside touching the support plate, each pair of membranes was secured between two lock rings positioned on either side of a support plate. Spacer plates were then inserted to ensure proper separation and alignment during testing. Figure 3.7 shows the RO membranes in practice.
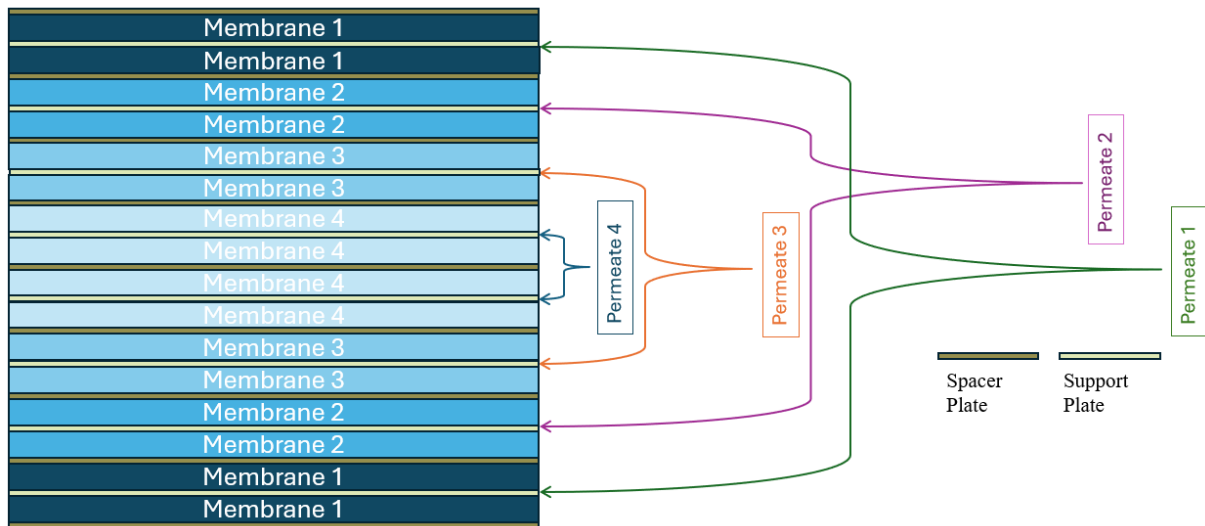


*Figure 3.5. Order of membranes in the membrane house of M20 TestUnit*

*Table 3.3. Permeate numbers for different NF and RO membrane type*

| Permeate | Membrane type (NF) | Membrane type (RO) |
|----------|--------------------|--------------------|
| 1 | NF90 | BW30 |
| 2 | NF270 | RO99 |
| 3 | NF99HF | RO98pHt$^{TM}$ |
| 4 | NF | RO90 |

*Figure 3.6. RO membranes in practice in the membrane house of M20 TestUnit, MemLab, Lund University*

The total volume of the water sample was calculated to be 8.755 L, including the dead volume of the system (1.255 L). Before conducting the experiments, it is vital to condition the membranes to ensure the removal of preservatives or contaminants introduced during storage or transportation, which was done by using Ultrasil 110 (ECOLAB) (liquid form). The cleaning protocol involved adding 26 mL of Ultrasil 110 to 8.755 liters of water (0.3% Ultrasil 110), recirculating the cleaning solution, and running the system for 30 minutes at a pressure of 5 bar with a final pH adjusted to 11 and the temperature set to 45°C, followed by pure water flux at 25°C and under a pressure of 9 bar (NF) and 15.5 bar (RO) for 30 minutes. Afterwards, membranes were separately treated with 0.25% Sodium Chloride (22 g) for RO and 0.20% Magnesium Sulphate (17.5 g) for NF, diluted in osmosis water. The NF membranes underwent a 30-minute run at 9 bar and 25°C, while the RO membranes ran for the same duration at 15.5 bar and 25°C, followed by electroconductivity tests for both the salt solution and the permeate. This particular step was implemented to confirm the integrity of the membranes, because, if the membranes are intact, there should be a minimal passage of salts into the permeate, resulting in low levels of electroconductivity. Again, the membranes were run for 30 minutes with pure water at 25°C and a pressure of 9 bar (NF) and 15.5 bar (RO), and the system was flushed.

During the experimental phase, the system was first completely drained and then refilled with 7.5 liters of drinking water from Sydvatten (Vombverket), adjusted to account for a calculated dead volume of 1.255 liters, plus an additional 200 mL for reference sampling, giving a total volume of 8.955 liters. To achieve a PFAS concentration of 1 µg/L in the water samples, 0.08955 mL of the stock solution (8.955 µg of PFAS) was added to the feed (8.955 L). All the calculation steps are provided in the Appendix.

During all experiments feed flow rate was constant at 8 L/min with membrane operating pressure set to 15 bar and 30 bar for all the NF and RO membranes, respectively, at a temperature of 30°C. The recovery rate was set to 50%, in the second run of the NF experiment, however, 70-75% water was recovered to ensure sufficient amount of water for sample collection. Samples were systematically collected from both the feed and permeate to evaluate membrane performance on the PFAS removal and the flux of permeate was monitored at the beginning and end of each experiment to estimate the fouling of the membranes. A picture of permeate collection is shown in Figure 3.7. The permeate fluxes of all the PFAS spiked water samples were recorded both manually and electronically. The following formula was used to calculate the flux:

$$J_{NF} = J_{RO} = \frac{\Delta V}{A_m \times \Delta t}$$

Here, J is the membrane flux, $A_m$ is the effective membrane area, $\Delta V$ is the volume collected, and $\Delta t$ is the collection time.
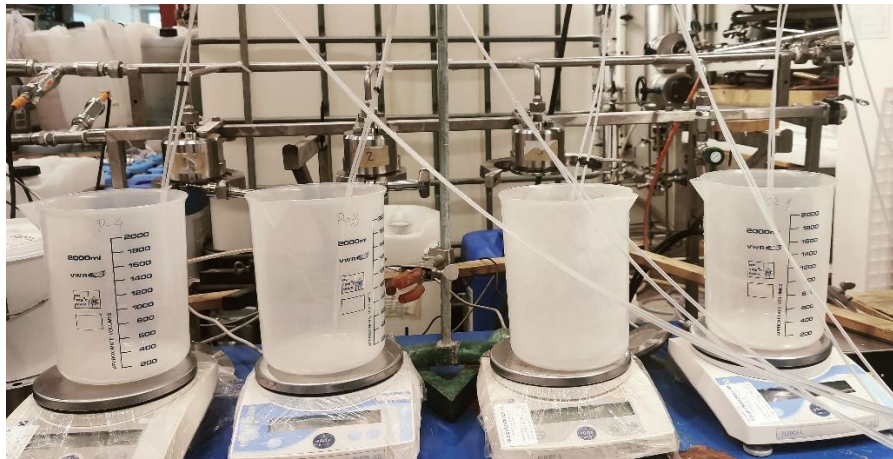


*Figure 3.7. Collection of four different permeates by four different membranes (NF and RO, separately), MemLab, Lund University*

In the triplicate experiments, at the end of each experiment, whether the membranes required cleaning was determined by filling up the feed tank with drinking water and comparing the flux with the initial flux of the previous experiment. If the flux was the same as earlier (+/-20%), no cleaning was needed, otherwise, the membranes were subjected to the same cleaning protocol as initially applied, ensuring they were maintained in optimal condition for subsequent testing. At the end of each group experiment, the membranes were cleaned by adding 26 mL of Ultrasil 110 to 8.755 liters of water (0.3% Ultrasil 110), recirculating the cleaning solution, and running the system for 30 minutes at a pressure of 5 bar, pH of 11 and a temperature of 45°C, followed by pure water flux at 25°C and under a pressure of 9 bar for NF and 15.5 bar for RO membranes for 30 minutes.

## 3.7 PFAS evaluation and water quality assessment

A total of 96 samples were collected throughout the experiments as shown in Figure 3.8 (48 for NF and 48 for RO) for the water analysis and PFAS testing, each sample had a volume of 200 mL. The samples are named with an E and S, where S represents the start and E represents end of the experiment. A detailed list of the sample names is given in the Appendix. A total of 72 samples were collected to evaluate PFAS concentrations in drinking water, with an equal split between nanofiltration (NF) and reverse osmosis (RO) samples (36 each). These samples were sent to the Swedish University of Agricultural Sciences (SLU) for PFAS analysis. The samples were taken at various stages of the experiments: before the experiments began (blank drinking water), during the experiments (reference: drinking water plus spike solution), feed at stable flux (both the beginning and end of the experiments), retentate, and each type of membrane permeate (at the be-ginning and end).

In addition, quality parameters of the water samples were also analysed during the second set of triplicate experiments (12 each for NF and RO). The water quality tests include Ion Chromatography, Inductively Coupled Plasma Optical Emission Spectrometry (ICP-OES), Carbon/Nitrogen (C/N) in water: Inorganic Carbon (IC) / Total Organic Carbon (TOC) / Total Nitrogen (TN) analysis of PFAS-spiked drinking water samples. Again, the samples were taken at different stages: before the experiments (blank drinking water), during the experiments (reference: drinking water plus spiked solution), feed at stable flux (both the beginning and end of the experiments), retentate, and permeates (at the beginning and end). Out of 96, 24 collected samples were sent to the Instrumental Chemistry Laboratory in the Department of Biology at Lund University for water quality analysis.



*Figure 3.8. Samples collected during RO membrane filtration, MemLab, Lund University*

# 4 Results and Discussion

This section contains the results and discussion of the findings from the membrane filtration focusing mainly on membrane flux, and water quality tests of PFAS-spiked drinking water samples. In addition to predicting the PFAS removal by the NF and RO membranes, these concentrations are compared with regulatory standards to assess potential health risks and water quality issues.

All the membranes used are cut into the same size to make them fit in the membrane house of the M20 system and the membrane area was calculated to be 0.027 $m^2$. The results of the electroconductivity tests confirmed the integrity of all the NF and RO membranes by significantly rejecting salts. Permeates are divided into four categories for four NF and RO membrane types for both the NF and RO membranes and pure water flux was checked to check the possibility of fouling of the membranes, which are presented in Table 4.1 and 4.2.

## 4.1 Pure water flux

During the triplicate experiments, pure water flux was observed after each test to confirm the permeability of the membranes. From the data presented in Table 4.1 and 4.2, it has been found that the difference in pure water flux between first-second and first-third run was below +/- 20% for all the permeates. This implies that both the NF and RO membranes did not require cleaning in between the triplicate experiments. In other words, it proves that the used NF and RO membranes did not show fouling during the experimental period.

*Table 4.1. Average pure water flux at the beginning of each NF membrane filtration*

| NF Test No. | Average Membrane flux: NF90 (Permeate 1) (L/m².hr) | Average Membrane flux: NF270 (Permeate 2) (L/m².hr) | Average Membrane flux: NF99HF (Permeate 3) (L/m².hr) | Average Membrane flux: NF (Permeate 4) (L/m².hr) |
|---|---|---|---|---|
| 1 | 210 | 443 | 412 | 132 |
| 2 | 214 | 442 | 413 | 128 |
| 3 | 218 | 436 | 401 | 128 |

*Table 4.2. Pure water flux at the beginning of each RO membrane filtration*

| RO Test No. | Average Membrane flux: BW30 (Permeate 1) (L/m². h) | Average Membrane flux: RO99 (Permeate 2) (L/m². h) | Average Membrane flux: RO98pHt™ (Permeate 3) (L/m². h) | Average Membrane flux: RO90 (Permeate 4) (L/m². h) |
|---|---|---|---|---|
| 1 | 155 | 165 | 222 | 378 |
| 2 | 140 | 144 | 203 | 356 |
| 3 | 131 | 138 | 192 | 339 |

The data analysis reveals intriguing trends in membrane performance. Notably, the difference in pure water flux between consecutive runs remained consistently below +/- 20% for all permeates, indicating minimal fouling and the absence of the need for inter-run cleaning.

## 4.2 NF membrane permeate flux

The average permeate fluxes of all three NF tests are calculated and presented in this section.

### 4.2.1 NF90 (Permeate 1)

In the case of Permeate 1 for nanofiltration membranes, the average flux was more or less same throughout the filtration period (see Figure 4.1). The error bars used in the graph are almost invisible meaning the mean values did not vary much from the true values of the individual runs. Therefore, it can be stated that no fouling was observed during the time of the experiment.

(Note: the errors bars could have been visible with a smaller Y-axis scale, however, to improve the comparison of the fluxes of all the NF membranes together, the same scale was maintained)
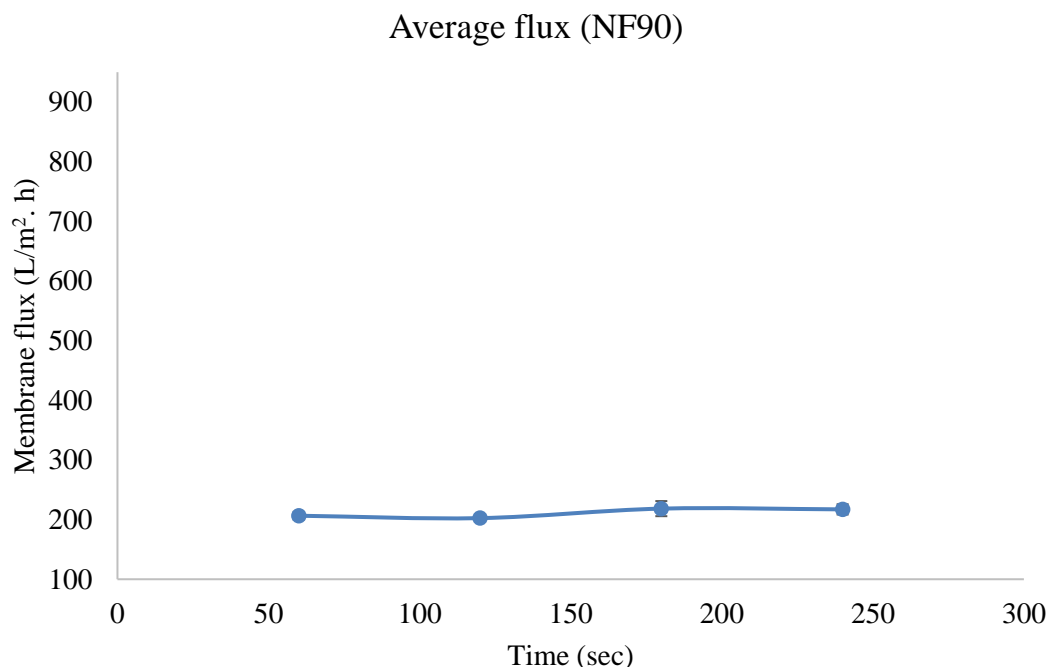


*Figure 4.1. Variation of average membrane flux over time for NF90 (Permeate 1), (mean of 3 consecutive runs for permeate 1), Time is in seconds and membrane flux is in L/m². h*

### 4.2.2 NF270 (Permeate 2)

In the case of NF270 (Permeate 2), the average membrane fluxes varied over time and there was flux drop at the second data point at around 200 seconds. This could be due to some measurement error or could also be because of the usual unstable flux behavior at the beginning of membrane filtration. However, the flux at the end of the graph showed that the flux was almost stable and that is why it can be stated that no fouling was evident during the experimental period. Moreover, the overlapping of the error bars towards the end of graph is also evident of no fouling.
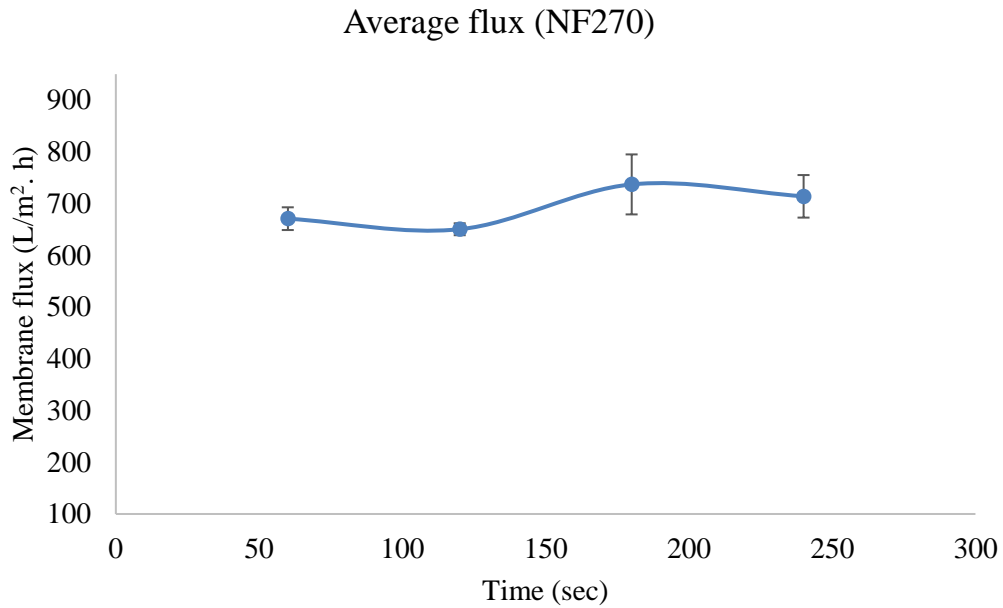
Average flux (NF270)

*Figure 4.2. Variation of average membrane flux over time for NF270 (Permeate 2), (mean of three consecutive runs of permeate 2), Time is in seconds and membrane flux is in L/m². h*

### 4.2.3 NF99HF (Permeate 3)
Similar to NF270, the average membrane fluxes of NF99HF (permeate 3) showed a similar type of behavior and it can be stated that there was no fouling for in NF99HF as well.
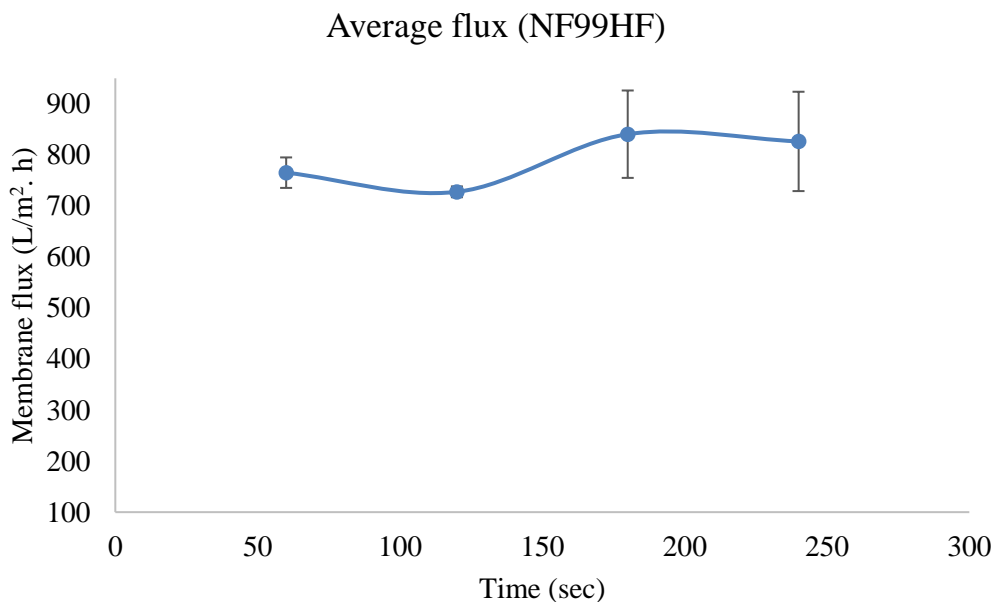


Average flux (NF99HF)

*Figure 4.3. Variation of average membrane flux over time for NF99HF (permeate 3), (mean of three consecutive runs of Permeate 3), Time is in minutes and membrane flux is in L/m². h*

### 4.2.4 NF (Permeate 4)

For NF (permeate 4), similar behavior could be seen as NF270 and NF99HF. The flux was more or less stable towards the end, so it can be stated that no fouling was evident during the experimental period.
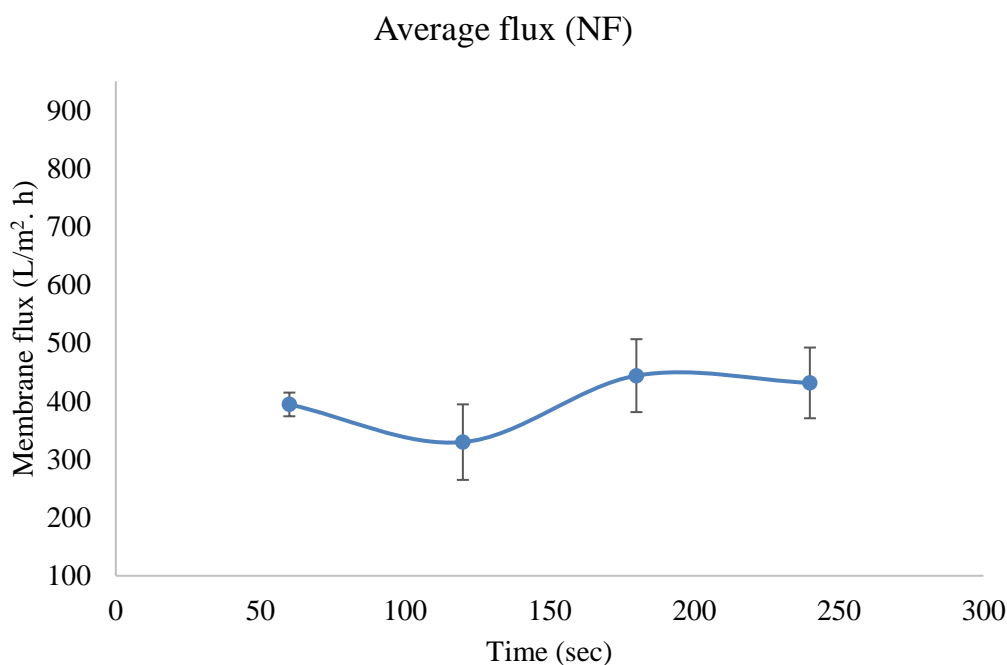
Average flux (NF)



*Figure 4.4. Variation of average membrane flux over time for NF (permeate 4), (mean of three consecutive runs of Permeate 4), Time is in minutes and membrane flux is in L/m². h*

The membrane flux variation of all the NF membranes with time indicates more or less stable fluxes during the experimental period, however, the experiments were very short. To provide a clearer idea about which NF membrane is the best among the four used, this study has also considered a comparative analysis (Figure 4.5). The comparison among different NF membrane types revealed variations in membrane flux behavior, with NF99HF consistently demonstrating the highest average flux values, followed by NF270, NF, and NF90. That is why NF99HF had the highest permeability, as membrane flux and permeability are directly proportional to each other as they were operated under the same conditions. However, a flux drop could be seen in all the membranes, except in NF90, which needs further investigation. Although NF90 showed the lowest flux rate, unlike the other NF membranes, its flux was more stable. Tang *et al.*, (2007) also observed exhibition of lower flux rates by NF90 than NF270. As the operating conditions were the same and the same feed was used for all NF the membrane types, the change in average flux rate could be due to the variation of membrane material compositions and pore sizes. Therefore, it can be said that NF99HF, with its higher average flux values, may be better suited for applications requiring high permeability. As NF90 exhibited the lowest flux vales, maybe due to its lower pore sizes, it is expected to have efficient PFAS removal rates.
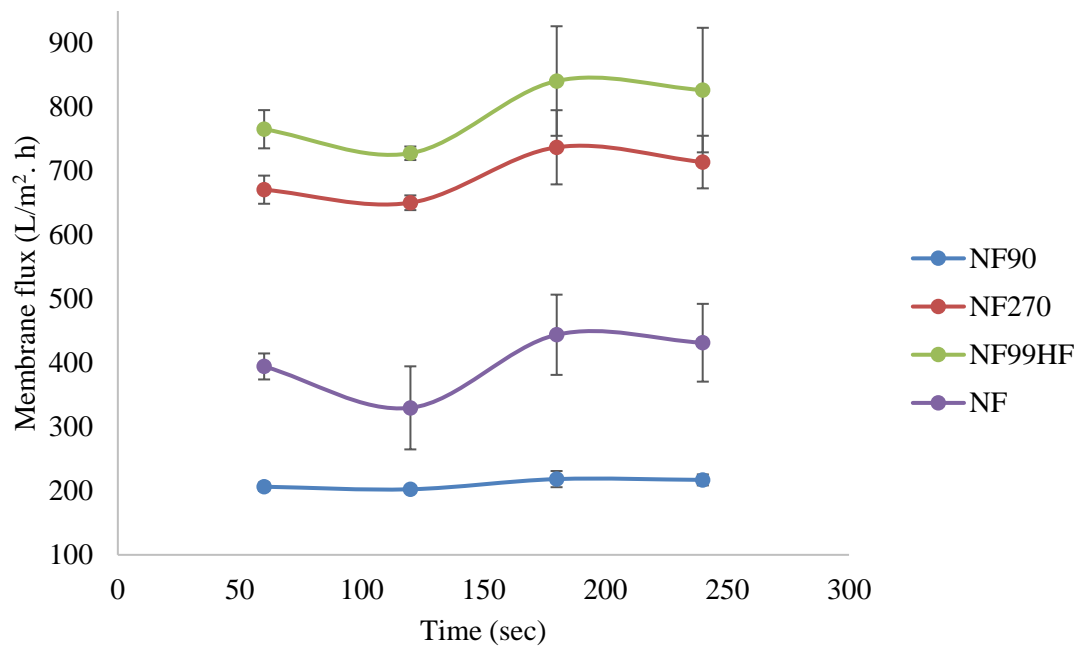
Figure 4.5. *Variation of average permeate flux over time for all NF membranes, time is in seconds and membrane flux is in L/m². h*

## 4.3 RO membrane permeate flux

The average permeate fluxes of all three RO tests are calculated and presented in this section.

### 4.3.1 BW30 (Permeate 1)

During the RO filtration process for BW30 (Permeate 1), the average flux remained relatively consistent throughout the filtration period. Although there was an initial peak in flux, it reached a stabilized phase after the first 150 seconds. The peak was maybe due to the unstable fluxes at the beginning. Despite the slight individual fluctuations, the error bars of the average fluxes in Figure 4.6 indicate minimal differences throughout the entire experiment. It also indicates that the uncertainties of the data are low. This consistency suggests that there was no significant fouling during the filtration process.
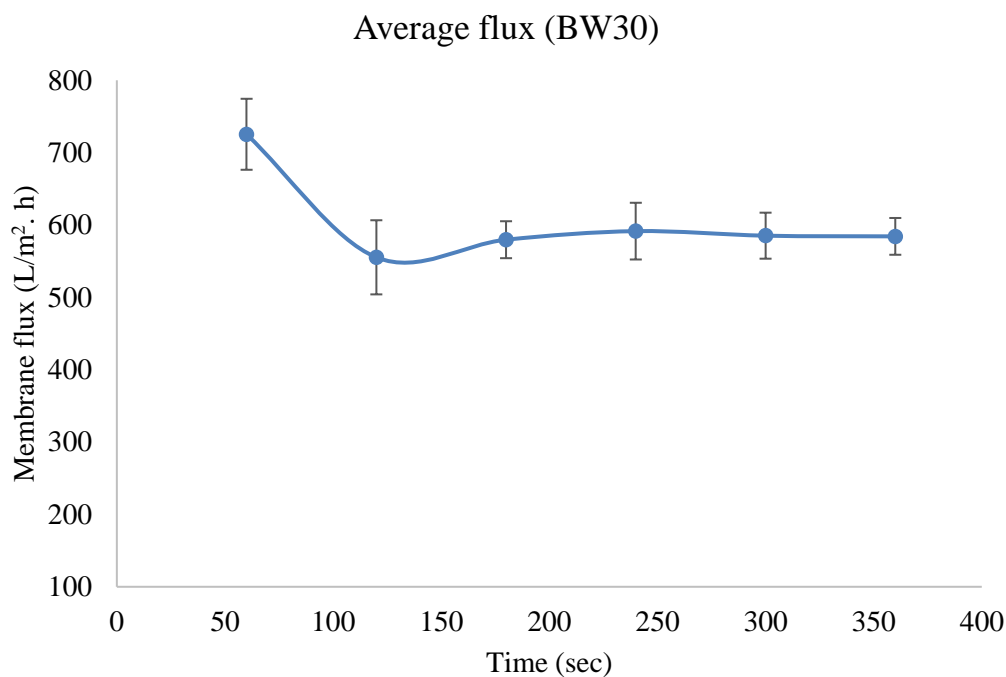


*Figure 4.6. Variation of average membrane flux over time for BW30 (permeate 1), (the mean of three consecutive runs of permeate 1), Time is in seconds and membrane flux is in L/m². h*

### 4.3.2 RO99 (Permeate 2)

For RO99 (Permeate 2), a slight fluctuation was noticed in the average membrane fluxes over the time compared to BW30 (see Figure 4.7). However, the average fluxes were more or less stable since the error bars are somewhat aligning. Moreover, the initial flux values for Permeate 2 were lower than Permeate 1.
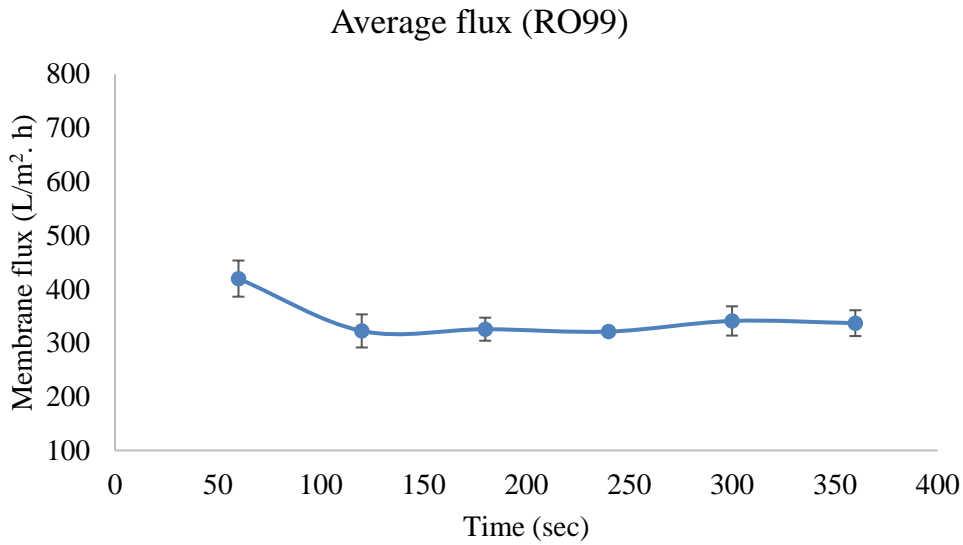
*Figure 4.7. Variation of average membrane flux over time for RO99 (permeate 2), (the mean of three consecutive runs of permeate 2), Time is in seconds and membrane flux is in L/m². h*

### 4.3.3 RO98pHt<sup>TM</sup> (Permeate 3)

In the case of RO98pHt<sup>TM</sup> (Permeate 3), the average membrane flux trend was somewhat similar to RO99 with less fluctuation. However, the overall flux rate was slightly lower (see Figure 4.8). The length of the error bars of the average membrane fluxes indicate that the uncertainties of the data are low and as they were nearly aligned indicating stability of flux values, it can be stated that no fouling was observed.



*Figure 4.8. Variation of average membrane flux over time for RO98pHt<sup>TM</sup> (permeate 3), (average is the mean of runs, Time is in minutes and membrane flux is in L/m². h*

### 4.3.4 RO90 (Permeate 4)

For RO90 (Permeate 4), similar behavior was recorded as RO98pHt[TM] including the overall flux rate and its behavior with time (see Figure 4.9). The length of the error bars of the average membrane fluxes indicate that the uncertainties of the data are low and as they were nearly aligned indicating stability of flux values, it can be stated that no fouling was observed.
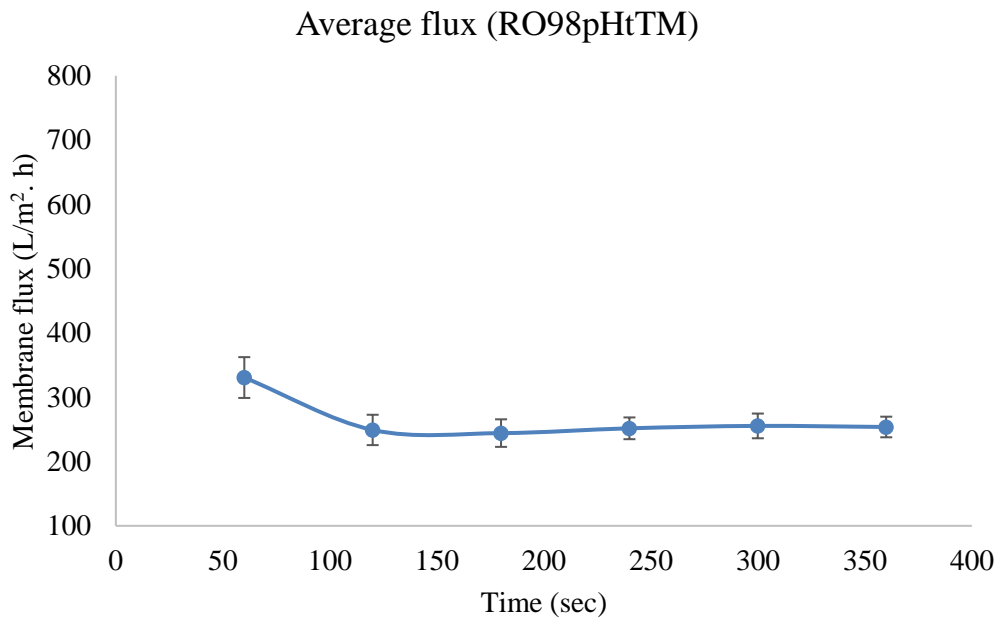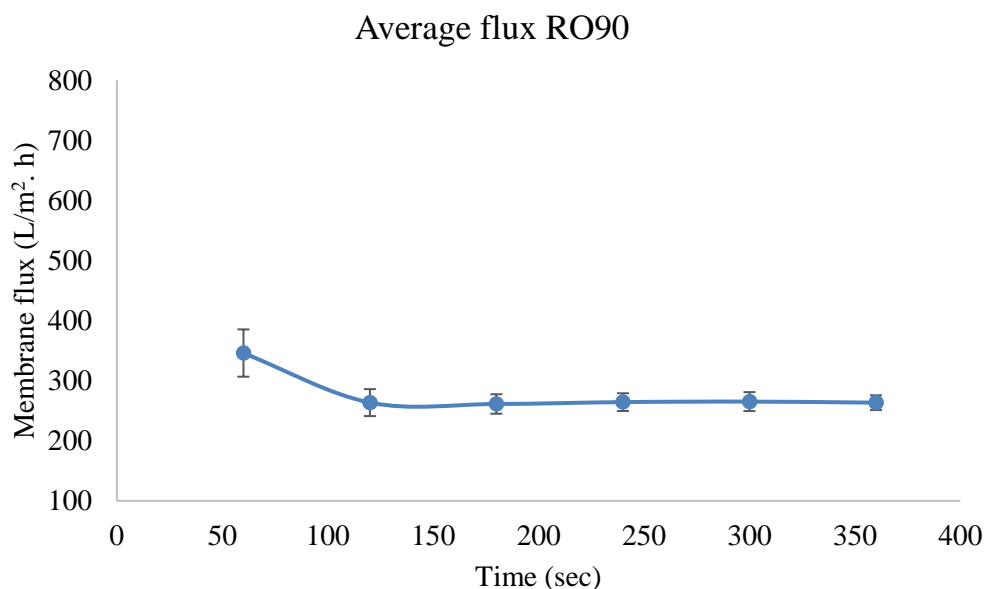


*Figure 4.9. Variation of average membrane flux over time for RO90 (permeate 4), (the mean of three consecutive runs), Time is in seconds and membrane flux is in L/m². h*

The average results of membrane fluxes for all the four types of RO indicated that there was no sign of fouling during the experiments. To check the best RO among the four membranes in the case of fouling, the mean flux values were compared (Figure. 4.10). BW30 consistently demonstrates the highest average flux values, followed by RO99, RO90, and RO98pHt[TM]. Given that the operating conditions were the same, factors like membrane material composition and membrane matrix can affect the performance of membranes. All the studied membranes showed satisfactory performance regarding flux rates, nevertheless, other factors i.e. removal of ions, organic matters should also be taken into consideration for a better prediction of their performance towards PFAS removal (see next section). Moreover, membranes with higher initial flux can face greater flux reduction due to increased hydrodynamic permeate drag at higher initial flux (Tang *et al.*, 2007). Similar behavior could be seen in BW30, which had an average initial flux of 725 L/m². h that decreased up to 580 L/m². h and became almost stable. Tang *et al.*, (2006) further demonstrated effective removal of PFOS by BW30, while maintaining a stable flux, and since BW30 in study also showed similar stable flux behavior, showing the low probability of fouling; it is expected to remove PFOS and similar chain-length PFAS efficiently. RO99, RO90 and RO98pHtTM are also anticipated to be effective in removing PFAS. However, there are currently no scientific studies available to confirm their effectiveness.
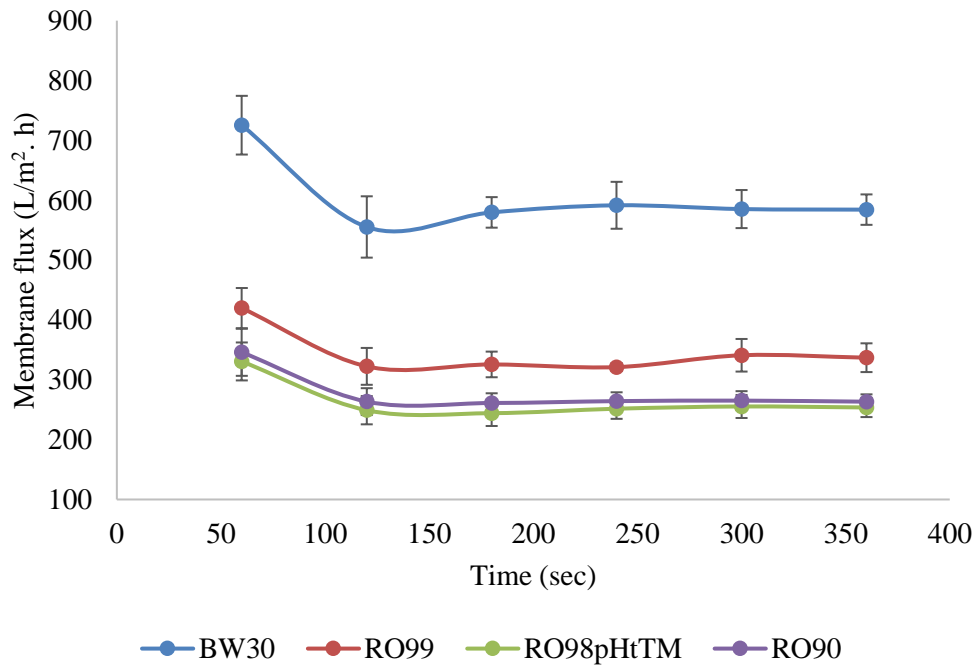
*Figure 4.10. Variation of average permeate flux over time for all the RO membranes i.e. BW30, RO99, RO98pHt$^{TM}$, RO90, Time is in seconds and membrane flux is in L/m². h*

## 4.4 Water quality analysis

The results of ion chromatography are divided into three parts i.e. removal of monovalent ions and divalent ions, and the removal efficiencies of NF and RO membranes are examined. The report will first present the removal of monovalent ions, followed by divalent ions and lastly trivalent ions, and afterwards the reduction of TOC from the samples.

### 4.4.1 Ion removal by NF membranes
This section explains the behavior of the NF membranes towards the removal of monovalent and divalent ions. Column diagrams are used to display the results of removal (%). Rejections of all the ions are displayed in Figure 4.11 (monovalent) and Figure 4.12 (divalent).

### *4.4.1.1 Potassium (K+)*

NF90 (NF90 (S) and NF90 (E)) showed moderate potassium ($K^+$) removal, with removal rates of 42.8-43.6%, reducing levels to 0.98-0.99 mg/L, respectively. NF270 (both NF270 (S) and NF270 (E)) had lower removal rates, with potassium levels at 1.4-1.5 mg/L, corresponding to 6.2-13.7% removal, respectively. NF99HF membrane demonstrated low to moderate efficiency, with levels reduced to 1.5 mg/L (S)-1.6 mg/L (E), translating to 9.4-16.5% removal. The NF membrane, on the other hand, showed mixed results with NF (S) achieving 19.4% reduction at a stable flux, whereas NF (E) indicated no removal.

### *4.4.1.2 Sodium (Na+)*

NF90 effectively reduced sodium concentrations to 1.5-1.6 mg/L, achieving high removal rates initially 84.7% and 86% at the end of the experiment. NF270, however, was much less effective, with sodium levels at 8.2 mg/L (S) and 10 mg/L (E), corresponding to 7.9-24.2% removal. The NF99HF membrane showed moderate removal efficiency, with sodium concentrations at 7.6 mg/L (S)-9.3 mg/L (E) and removal rates of 14.1-29.6%, respectively. The NF membrane displayed highly variable performance, with one sample showing 36% removal at the beginning and eventually no removal as presented in Figure 4.11.

### *4.4.1.3 Fluoride (F-)*

NF90 achieved high fluoride removal rates, reducing concentrations to 0.005-0.008 mg/L, corresponding to 90.9% removal rates which was increased up to 94.3% at the end. NF270 showed moderate efficiency, reducing fluoride concentrations to 0.040-0.056 mg/L, achieving 36.4% (S)-54.5% (E) removal. Effective removal of fluoride was recorded by NF99HF membrane, lowering down the levels at 0.037 mg/L-0.058 mg/L, equal to rejection rates of 34.1% (S) and 58% (E). However, the performance of NF membrane showed a negative trend with higher removal at the beginning (86.4%) and moderate removal at the end (47.7%).

### *4.4.1.4 Chloride (Cl-) Removal*

Both the NF90 samples i.e. NF90 (S) and NF90 (E) showed high efficiency in chloride removal, reducing concentrations to 2.08 mg/L and 2.18 mg/L, achieving removal rates of 92.3% and 92.7%, respectively. NF270 membrane demonstrated lower efficiency, with chloride levels reduced to 24.62 mg/L (S) and 28.36 mg/L (E), corresponding to a removal rate of 13.6% and 21.1%, respectively. NF99HF membrane showed moderate removal efficiency of Chloride ions, by reducing the ion concentration to 21.25 mg/L (S) and 26.50 mg/L (E), equal

to removal rates of 25.4% at the start and became 39.2% at the end. The removal rates for NF membrane was around 40% at the start and eventually showed no removal towards the end of the experiment.

### 4.4.1.5 Nitrate (NO$_3^-$)

NF90 showed high nitrate removal efficiency, reducing concentrations to 0.138 mg/L-0.155 mg/L, achieving removal rates of 65.6% (S) and 69.3% (E). NF270, however, showed very low rejections, almost no change from the initial concentration. NF99HF performed moderately, reducing nitrate to 0.411 mg/L (8.7%) at the start, which increased up to 0.436 mg/L (9%). Similar to NF270, the NF membrane also showed no removal at the end of the experiment (E).
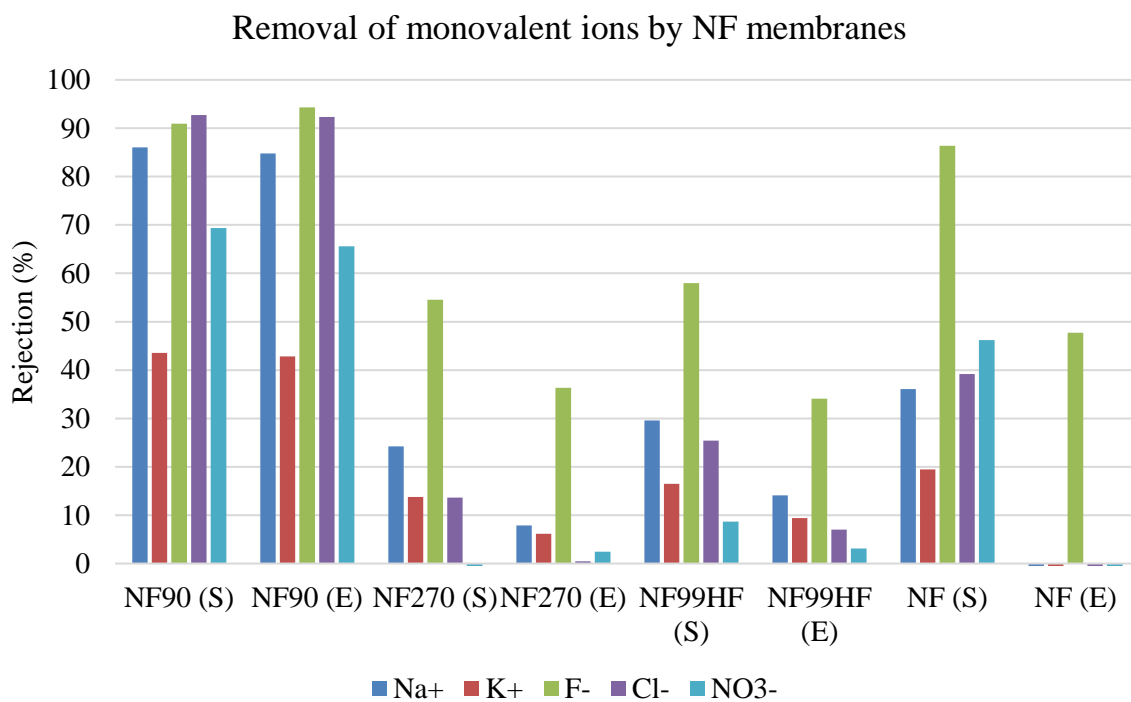


*Figure 4.11. Rejection (%) of monovalent ions (Na$^+$, K$^+$, F$^-$, Cl$^-$ and NO$_3^-$) in the water samples by NF membranes at different stages of membrane filtration operation*

### 4.4.1.6 Calcium (Ca$^{2+}$)

The NF membranes demonstrated variable efficiency in calcium removal. The NF90 membrane showed high removal rates for both the start (S) and end (E) samples, reducing calcium concentrations from 18.259 mg/L to around 2.268 mg/L, achieving approximately 87.5% removal. Conversely, the NF270 membrane was less effective, reducing calcium levels to about 12 mg/L (S)-15 mg/L (E), with removal rates of only 17.9%-34.4%, respectively. The

NF99HF membrane exhibited moderate removal efficiency, lowering calcium concentrations to 10 mg/L at the beginning and further down to 13 mg/L at the end, corresponding to 27.6%-44.5% removal. The NF membrane showed significant variability, with a concentration of 6.6 mg/L (=63.6% removal) at the beginning (S) which was increased up to 13 mg/L (E) with a removal of 27.9%.

### 4.4.1.7 Magnesium (Mg²⁺)

The NF90 membrane excelled in magnesium removal, achieving reductions to around 0.05 mg/L = 96% throughout the process. The NF270 membrane showed moderate efficiency, lowering magnesium to 0.94 mg/L (S)-1.31 mg/L (E), with removal rates of 15.9%-39.6%, respectively. The NF99HF membrane's performance was intermediate, reducing magnesium to 0.77 mg/L (S) and 1.12 mg/L (E), corresponding to a removal rate of 27.9% (S) and 50.2% (E). The NF membrane again showed variability, with high removal in at the start (S) (84.3%) and moderate removal in the end (E) (57.4%).

### 4.4.1.8 Sulfate (SO₄²⁻)

NF90 effectively reduced sulfate concentrations to 0.06 mg/L throughout the process, achieving removal rates of 96%. NF270 also showed effective sulfate removal, reducing levels to 0.123 mg/L-0.168 mg/L, corresponding to 88.8%-91.8% removal at the start and end, respectively. Similarly, NF99HF membrane exhibited high removal efficiency, with sulfate levels at 0.11 mg/L in both (S) and (E) with a removal rate of 92%. The NF membrane displayed the highest removal, reducing sulfate to 0.036 mg/L (S)-0.052 mg/L (E), achieving 96.5%-97.6% removal, respectively.
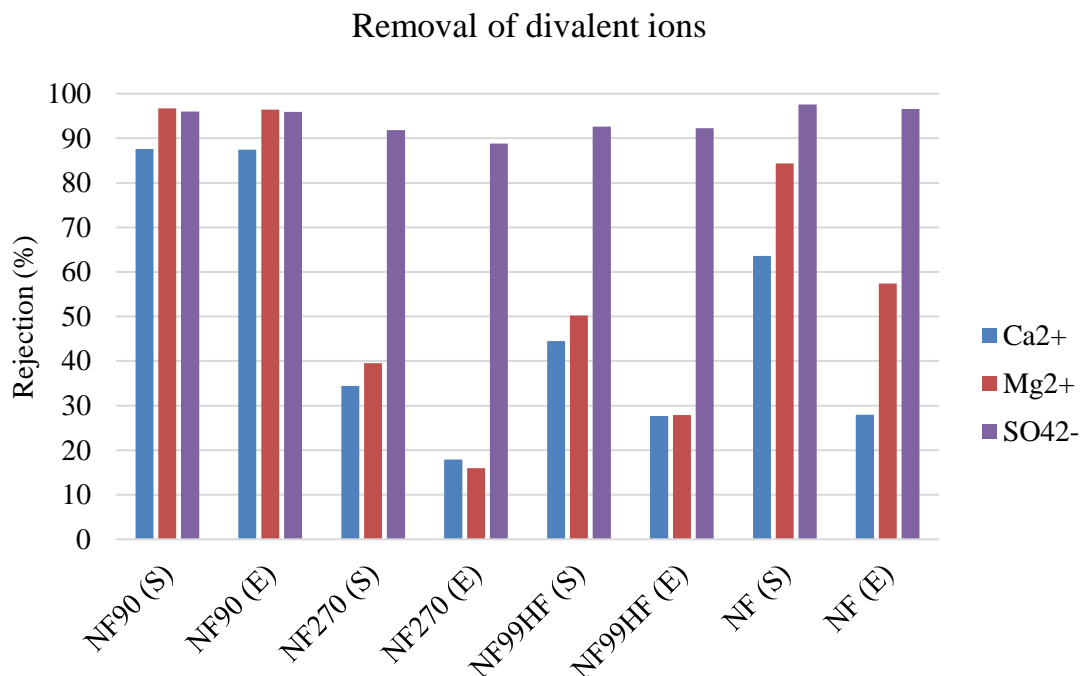


*Figure 4.12. Rejection (%) of divalent ions (Ca²⁺, Mg²⁺, and SO₄²⁻) in the water samples by NF membranes at different stages of membrane filtration operation*

Overall, NF membranes performed better in the removal of divalent ions than monovalent. The results indicate the superior ion rejection capability of both BW30 and NF90, which is crucial for dealing with PFAS, which are known for their persistence and difficulty in removal due to their chemical stability. The NF90 membrane showed a similar removal percentage as Zouhri et al., (2017), with a removal of $Na^+$ and $Cl^-$ ions around 90%. The study further mentioned that the highest rejection by NF90 was observed due to its nearly similar characteristics as RO membranes. The NF99HF membrane also showed significant reductions but was slightly less effective than NF90 in the removal of divalent ions, whereas the difference is much higher for monovalent ion removal. NF270 performed moderately for both monovalent and divalent ions. The results obtained for NF270 membranes reflected somewhat the same behavior as obtained by Zouhri et al., (2017). The superior performance of NF90 can be attributed to its tighter membrane pore size, which effectively filters out smaller ions. The membrane composition can also be a matter of fact. Therefore, NF99HF has shown higher permeability than NF90 (see Figure 4.5). Overall, it can be stated that considering the wide chain-length range of PFAS, NF90 would be better if cleaning is performed regularly. NF99HF, while still effective, the slightly larger pores compared to NF90 might result in marginally lower PFAS rejection rates. However, the difference might not be significant depending on the specific PFAS compounds and their molecular sizes.

**4.4.2 Ion removal by RO membranes**

This section explains the behavior of the RO membranes towards the removal of monovalent and divalent ions. Column diagrams are used to display the results of removal (%). Rejections of all the ions are displayed in Figure 4.13 (monovalent) and Figure 4.14 (divalent).

### 4.4.2.1 Potassium (K+)

All the RO membranes (BW30, RO99, RO98pHt$^{TM}$ and RO90) demonstrated moderate removal of potassium (K$^+$) ion, decreasing the concentration to around 0.9 mg/L, corresponding to a removal of around 46%, both at the start and end of the experiment.

### 4.4.2.2 Sodium (Na+)

All the RO membranes achieved high sodium (Na$^+$) removal efficiency. The BW30 membrane reduced sodium levels to around 1 mg/L, corresponding to removal of 91% Na, throughout the process. Similarly, RO99, RO98pHt$^{TM}$ and RO90 showed more or less the same rejection efficiency (around 90%).

### 4.4.2.3 Fluoride (F-)

In case of F$^-$, the concentration was below detection limit (BDL) for almost all types of RO membranes, except for RO99 at the beginning (S) that showed a concentration of 0.001 mg/L and removal percentage was 99%, which again lowered down to below detection limit at the end (E). For the concentrations BDL, the removal was considered as 100% (see Figure 4.13)

### 4.4.2.4 Chloride (Cl-)

Similarly, chloride was also removed significantly throughout the experiment by all the RO membranes. All of them (BW30, RO99, RO98pHt$^{TM}$ and RO90) showed removal of 96% of Cl$^-$ in the permeates by reducing the Cl$^-$ concentration to 0.7 mg/L-1.2 mg/L.

### 4.4.2.5 Nitrate (NO3-)

In the case of nitrate (NO$_3^-$), the concentration was BDL at the start for BW30, RO99 and RO98pHt$^{TM}$ membranes (removal = 100%), however, at the end of the experiments, they showed an increase in NO$_3^-$ concentrations in the permeate (BW30 = 0.09 mg/L = 80% removal, RO99 = 0.03 mg/L = 95% removal, and RO98pHt$^{TM}$ = 0.1 mg/L = 78% removal). The NF membrane, on the other hand, performed moderately with a removal of 70%-74% removal by reducing the NO$_3^-$ concentration to 0.12 mg/L-0.14 mg/L, respectively in the beginning (S) and end (E) of the filtration process.
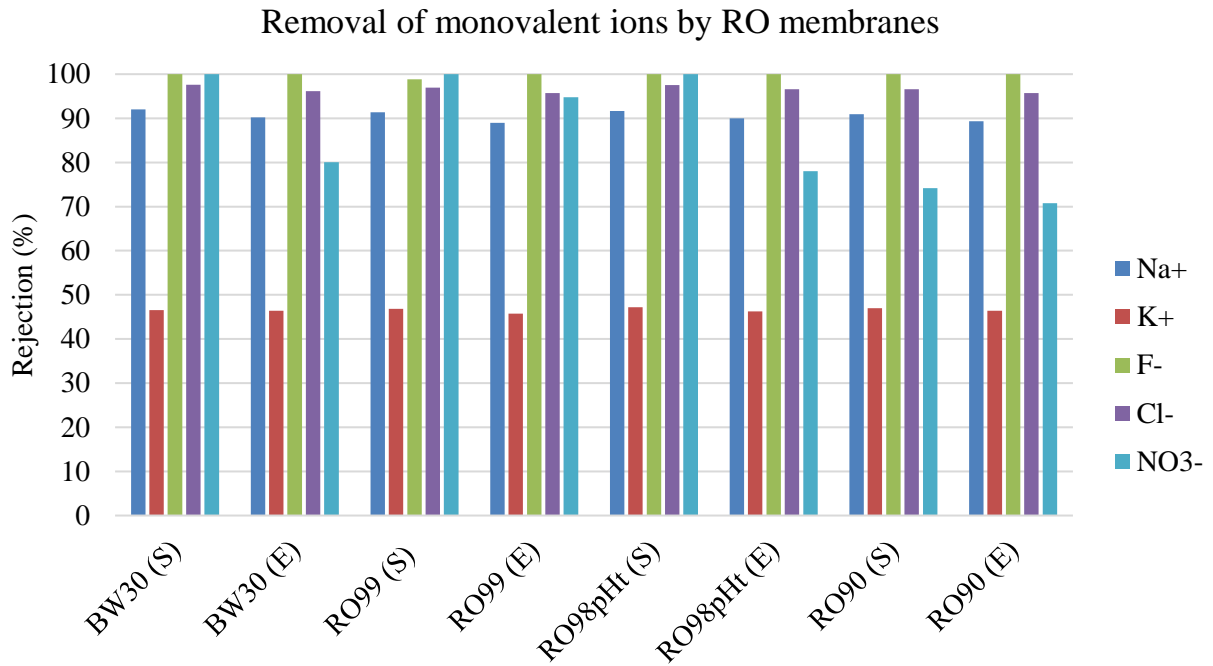
*Figure 4.13. Rejection (%) of monovalent ions ($Na^+$, $K^+$, $F^-$, $Cl^-$ and $NO_3^-$) in the water samples by RO membranes at different stages of membrane filtration operation*

### 4.4.2.6 Calcium ($Ca^{2+}$)

The RO membranes showed significant removal of calcium ion ($Ca^{2+}$) throughout the process, by lowering down the $Ca^{2+}$ concentration to around 2 mg/L with a removal of 93% for all the membranes (BW30, RO99, RO98pHt$^{TM}$ and RO90).

### 4.4.2.7 Magnesium ($Mg^{2+}$)

All the RO membranes (BW30, RO99, RO98pHt$^{TM}$ and RO90) showed excellent removal of magnesium ion ($Mg^{2+}$). A removal of 98% was observed throughout the process by all the RO membranes with a decrease in $Mg^{2+}$ concentration to 0.03 mg/L.

### 4.4.2.8 Sulfate ($SO_4^{2-}$)

Sulfate ($SO_4^{2-}$) removal was between 98%-99% throughout the filtration process, with BW30 showing the maximum removal. The concentration of $SO_4^{2-}$ was decreased up to 0.01 mg/L by BW30 and 0.03 mg/L by all the other RO membranes (BW30, RO99, RO98pHt$^{TM}$ and RO90).
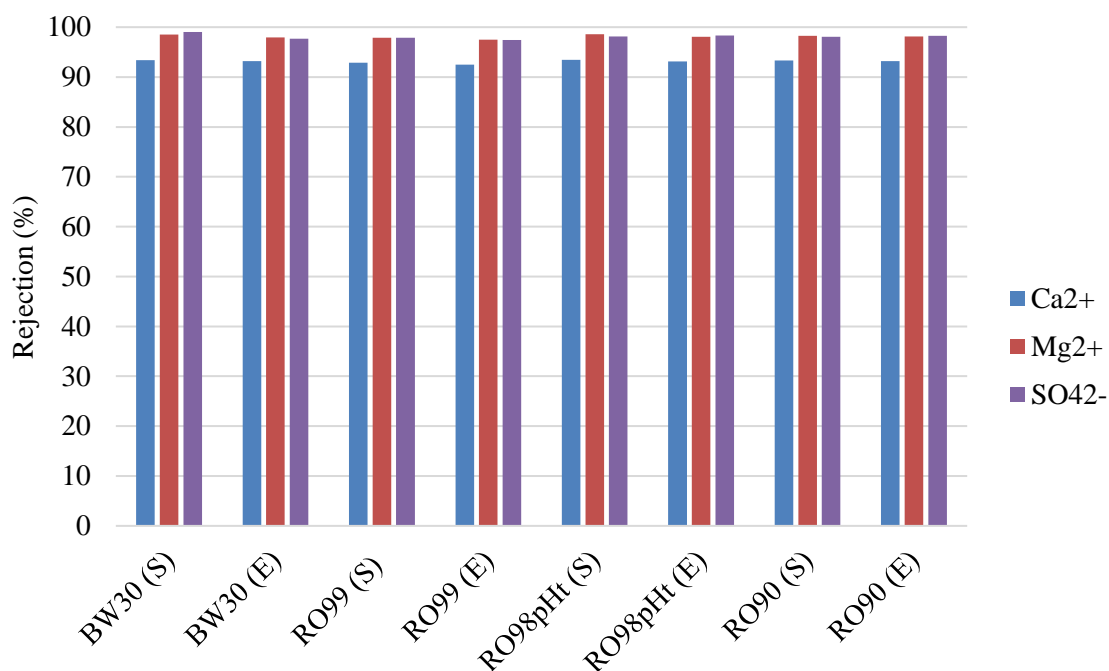
44

## Removal of divalent ions



*Figure 4.14. Rejection (%) of divalent ions ($Ca^{2+}$, $Mg^{2+}$, and $SO_4^{2-}$) in the water samples by RO membranes at different stages of membrane filtration operation*

In terms of RO membranes, all the membranes exhibited remarkable ion rejection capabilities, with the concentration of many ions reduced to nearly negligible levels. All the RO membranes demonstrated outstanding performance by lowering down the concentrations of Sodium ($Na^+$), Magnesium ($Mg^{2+}$), Calcium ($Ca^{2+}$), and the rest of the ions considered in this study to great extents with many of them showing near-complete removal of ions like fluoride, with concentrations below detection limits (BDL) in most samples. BW30 showed maximum removal of all the anions and cations, including $Na^+$ and $Cl^-$ >90%, at the same time maintained a higher membrane flux. Zouhri et al., (2017) also found a removal of more than 90% for anions like $Na^+$ and $Cl^-$ by BW30. More than 99% removal was recorded for $Na^+$, $Ca^{2+}$, $Mg^{2+}$, $Cl^-$, $NO^{3-}$, and $SO_4^{2-}$ by BW30 membrane according to Ruiz-García et al., (2020). Although RO90 and RO98pHt™ resulted in excellent removal percentage, their average fluxes were much lower than BW30. Factors like membrane pore size and membrane composition material can affect the performance of the membranes. Overall, it can be stated that BW30 is the best among the four RO membranes considered in this study, which highlights their effectiveness in treating PFAS-contaminated water. The other RO membranes also are expected to show efficient removal of PFAS, even though permeability will be lower than BW30.

### 4.4.3 Removal of Total organic carbon (TOC) by NF and RO membranes

Among the NF membranes, NF90 exhibited relatively higher Total Organic Carbon (TOC) removal efficiencies compared to the other NF membranes. Although NF99HF showed a removal of 30% at the start, it fell to almost 22% by the end. From Figure 4.15, only NF90 showed a consistent removal while for the other NF membranes, the removal efficiency varied all the time. Since the operating conditions were similar for all NF membranes, the differences in removal efficiencies can be attributed to the membrane properties i.e. material composition and membrane pore size. NF90 membranes have denser pore size compared to NF270 or NF99HF or NF, facilitating a comparatively higher removal organic molecules, including TOC. Similarly, maximum removal was found to be 44% by RO membranes. Slightly better than NF membranes due to their more compact composition, with removal of around 35% TOC by all the RO membranes except BW30, which showed around 30% removal. Among the four types of RO studied, RO90 performed the best in the removal of TOC by achieving a removal of around 44%. However, overall removal of TOC is remarkably low for all the membranes and further investigation is needed to find out the reason behind this.
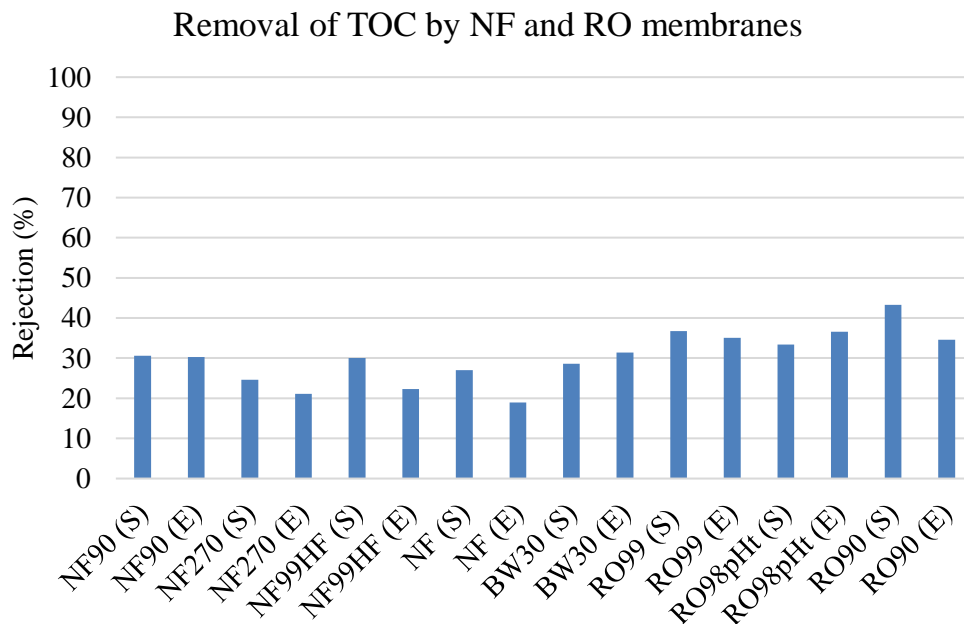


*Figure 4.15. Rejection (%) of TOC present in water samples by all the NF and RO membranes*

## 4.5 Comparative analysis between NF and RO membranes

### 4.5.1 Membrane flux
Overall, the flux rates of both NF and RO membranes indicated stability over time. Comparing the average initial flux values, two of the NF membranes exhibited an initial flux of >700 L/m$^2$. h, whereas only one RO reached a flux value of 700 L/m$^2$. h. This indicates that NF membranes have better permeability compared to RO membranes. Especially BW30, showing a flux drop of around 140 mg/L. Higher initial flux leads to higher removal of PFAS, however, at the same time, the reduction of flux can be more severe when the initial flux is high (Boonya-atichart, Boontanon and Boontanon, 2018, Tang *et al.*, 2006). This can be seen in BW30, as the flux decreased significantly, however, this also points that the PFAS removal should be higher by BW30. Operational conditions, including transmembrane pressure and crossflow velocity, also impact membrane flux, and so membrane fouling and cleaning (Jin et al., 2021). Higher operating pressures and crossflow velocities can help prevent fouling by promoting shear-induced detachment of foulants from the membrane surface (Mahlangu *et al.*, 2023). RO membranes operate under higher pressures compared to NF membranes. Although RO membranes need more pressure, and they showed lower flux. This could be due to their smaller pore size that consequently requires higher pressure and is more suitable in removing pollutants, but at the same time might undergo clogging or fouling, requiring more frequent cleaning than NF membranes. According to the experiments conducted by Naidu et al. (2015) and Zouhri et al., (2017), it was demonstrated that although the flux improved with increasing pressure, nanofiltration (NF) consistently exhibited higher flux than reverse osmosis (RO) at equivalent pressure levels due their relatively loose structure. Naidu et al., (2015) and Couto *et al.*, (2020) have also shown that NF membranes are better that require comparatively lower pressure but results in high flux, making the membranes more permeable.

Although the initial PFAS concentration was the same and the same tap water was used, there remains a high likelihood of variation in feed composition, which can lead to differences in flux rates. However, it is improbable that these variations in feed composition would significantly impact the flux. The extent of variation in feed composition is also unlikely to be vast enough to account for major changes in flux. Furthermore, the effectiveness of cleaning protocols between runs can vary, affecting the removal of foulants from the membrane surface. Although the data indicates that cleaning was not required between triplicate experiments, variations in cleaning protocols and efficiency may still impact membrane fouling and cleaning behavior.

### 4.5.2 Water quality
The water quality analysis data indicates that both NF and RO membranes can substantially reduce monovalent and divalent ion concentrations, which are proxies for their ability to handle PFAS. RO membranes have been proven to be more efficient than NF, due to their smaller pore size and chemical properties. Particularly BW30 is effective in significantly reducing these contaminants. After comparing the results of water quality analysis, it is confirmed that both NF and RO membranes are effective enough towards the removal of ions from water, and matches with the findings by Naidu et al., (2015). While highly effective in contaminant removal, RO-treated water often lacks essential minerals like calcium, sodium, and potassium (Bolisetty, Peydayesh and Mezzenga, 2019). This mineral depletion can be a limitation of RO membranes for drinking water purposes, as maintaining certain levels of these ions is important for health, as per *WHO/EU drinking water standards, 2024* (Table 4.3). Therefore,

the mineral retention capability of NF membranes makes them more suitable as they maintain the drinking water standards while also providing an efficient removal of contaminants. Mirbagheri *et al.*, (2016) also mentioned successful removal of ions by NF (NF90) and RO (BW30) membranes. Nevertheless, the RO membranes seemed more promising as highly effective in treating PFAS-contaminated water.

*Table 4.3. Standard ion concentrations allowed in drinking water decided by World Health Organization (WHO), and European Directives*

| Ions (mg/L) | WHO | EU Standards | Reference |
|---|---|---|---|
| **Boron (B)** | 0.3 | 1.0 | |
| **Calcium (Ca)** | 100 | -- | |
| **Chromium (Cr)** | 0.05 | 0.05 | WHO-EU-water- |
| **Iron (Fe)** | -- | 2 | standards, 2024 |
| **Magnesium (Mg)** | 50 | -- | |
| **Sodium (Na)** | 200 | 200 | EU Drinking water |
| **Chlorine (Cl)** | 250 | 250 | regulations, 2023 |
| **Fluorine (F)** | 1.5 | 1.5 | |
| **NO$_3$-N (Nitrate)** | 50 | 50 | |
| **SO$_4$-S (Sulphate)** | 500 | 250 | |

## 4.6 Prediction of PFAS removal

As previously mentioned, due to time constraints, PFAS analysis was not included in this report. However, based on prior studies on PFAS removal, a table (Table 4.5) has been created to list the predicted removal rates of PFAS by the 8 membranes considered in this report. This will facilitate future accuracy testing of the samples prepared for this study. Additionally, all the RO-treated water samples are expected to have efficient PFAS removal.

*Table 4.5. Predicted PFAS Removal Rates Based on Previous Studies*

| PFAS type | NF90 Removal rate (%) | NF270 Removal rate (%) | BW30 Removal rate (%) | Reference |
|---|---|---|---|---|
| **PFOS** | 90-99 | 90-99 | 99 | |
| **PFHxA** | 98.3 | 78 | 99.7 | (Tang *et al.*, 2007) |
| **PFOA** | 98.3 | $\geq 95$ | -- | (C. J. Liu *et al.*, |
| **PFBS** | 98.3 | 55.4 | -- | 2021) |
| **PFHxS** | 98.3 | $\geq 95$ | -- | (Safulko *et al.*, 2023) |
| **PFHpA** | -- | $\geq 95$ | -- | |
| **6:2 FTSA** | -- | $\geq 95$ | -- | |

# 5 Conclusions

PFAS contamination is a pervasive issue, with these substances found globally in several water sources despite regulatory efforts to limit their presence. The persistence and widespread distribution of PFAS highlights the significant challenge they pose to environmental health and safety. The contamination of drinking water with PFAS has been documented worldwide, affecting groundwater and surface water sources across diverse geographical regions. Different regions have varying levels of contamination, influenced by local industrial activities, regulatory measures, and historical usage patterns of PFAS-containing products. The health risks associated with PFAS exposure have led to the implementation of stringent regulations and guidelines by various countries and international organizations, including the EU Drinking Water Directives, the U.S. EPA, and the WHO. These limits reflect the severity of PFAS impacts on human health and the environment, necessitating stringent monitoring and control measures. Countries have tailored their regulations based on specific contamination scenarios and national priorities, resulting in different guidelines aimed at mitigating PFAS risks.

Effective removal of PFAS from drinking water is critical to mitigating their impact on public health. Membrane filtration technologies, particularly nanofiltration (NF) and reverse osmosis (RO), have proven effective in removing PFAS from water. These techniques offer high removal rates for a wide range of PFAS compounds, with RO membranes generally providing higher rejection rates due to their denser active layers. RO membranes can effectively reject over 99% of both long-chain and short-chain PFAS. NF membranes are also effective, particularly for long-chain PFAS. However, these membrane's efficiency can be influenced by operational conditions, transmembrane pressure, temperature, and feed concentration, as well as membrane properties like surface charge, pore size, and hydrophilicity. The removal mechanisms primarily involve steric exclusion and electrostatic interactions, which are affected by factors such as pH, ionic strength, and the presence of natural organic matter.

This study predicted the performance of nanofiltration (NF) and reverse osmosis (RO) membranes in removing PFAS from drinking water in a lab-stack unit, by analysing membrane flux and water quality, particularly ion removal and potential fouling. No fouling was observed during the experimental period; however, the period was very short, and the source was drinking water that already had lower contaminant concentrations. NF membranes demonstrated varying performances, as shown in Figure 4.5, NF90 had the lowest flux rates but showed consistent stability. Notably, NF99HF showed the highest permeability, making it suitable for high-flux applications, although NF90, despite its lower flux, is likely more efficient for PFAS removal due to its smaller pore sizes. In Figure 4.10, RO membranes, specifically BW30, showed the highest flux values, followed by RO99, RO90, and RO98pHtTM. BW30 demonstrated stable flux, indicating minimal fouling, and generally, all RO membranes exhibited minimal fouling, with BW30 being the most consistent performer.

The ion removal efficiencies of NF90 and BW30 membranes (removal rates over 90%) indicate their potential to meet regulatory standards for PFAS and other contaminants in drinking water, thereby mitigating potential health risks. The performance of NF and RO systems is influenced by various factors, including the specific characteristics of the feedwater, operational conditions, and the properties of the membranes used. Additionally, as RO-treated water had very low essential mineral concentration, this report recommends using NF mem-

branes while dealing with drinking water, or implementation of post-treatment strategies if RO is used.

While this study did not observe fouling in the membranes during its short-term experimental period and with drinking water samples already relatively low in contaminants, it is important to acknowledge the potential for fouling over extended usage. Membranes typically develop fouling over time, necessitating ongoing maintenance and monitoring. Additionally, it is extremely important to improve the monitoring of PFAS fate to mitigate the overall effect of PFAS in drinking water sources and thereby the human health. Therefore, some future research is recommended in the following section, including long-term membrane performance under real-world conditions and advancing the overall performance of membrane filtration.

# 6 Future research

Future research should focus on long-term studies to understand the fate of PFAS in order to control the spread of chronic health effects through it. Drinking water treatment technologies need development for efficient PFAS removal, including comprehensive environmental monitoring, which will help track PFAS levels, identify hotspots, and assess regulatory effectiveness. There should also be greater standardization over water-related regulations across regions and countries through comparative studies and developing risk assessment models for cumulative PFAS effects. Investigating climate change impact on PFAS distribution, enhancing public awareness, and fostering interdisciplinary collaborations are essential. Economic and social impact analyses of contamination and remediation efforts are needed to ensure cost-effective and sustainable solutions, ultimately protecting public health and water resources.

While nanofiltration and reverse osmosis membranes both demonstrate high efficacy in contaminant removal, each type has its advantages and limitations, as evidenced in this study. Future research should focus on addressing the challenges associated with membrane fouling and the operational and maintenance costs of NF and RO membranes, since membranes usually tend to develop fouling after a certain period of time. Additionally, sustainable solutions for the disposal and treatment of concentrated membrane retentate need to be developed to ensure the real-world application of membrane filtration in removing PFAS. Further in-depth investigations under varying operational conditions are necessary to determine the longevity, stability, and practicality of these membranes for full-scale water treatment plants.

# 7 References

Abubackar, H.N. *et al.* (2019) '2.31 - Gas-Phase Bioreactors', in M. Moo-Young (ed.) *Comprehensive Biotechnology (Third Edition)*. Oxford: Pergamon, pp. 446–463. Available at: https://doi.org/10.1016/B978-0-444-64046-8.00142-7.

Ahmed, M.A., Amin, S. and Mohamed, A.A. (2023) 'Fouling in reverse osmosis membranes: monitoring, characterization, mitigation strategies and future directions', *Heliyon*, 9(4), p. e14908. Available at: https://doi.org/10.1016/j.heliyon.2023.e14908.

Appleman, T.D. *et al.* (2013) 'Nanofiltration and granular activated carbon treatment of perfluoroalkyl acids', *Journal of Hazardous Materials*, 260, pp. 740–746. Available at: https://doi.org/10.1016/j.jhazmat.2013.06.033.

Arinaitwe, K. *et al.* (2021) 'Perfluoroalkyl substances (PFASs) in the Ugandan waters of Lake Victoria: Spatial distribution, catchment release and public exposure risk via municipal water consumption', *Science of The Total Environment*, 783, p. 146970. Available at: https://doi.org/10.1016/j.scitotenv.2021.146970.

Blake, B.E. and Fenton, S.E. (2020) 'Early life exposure to per- and polyfluoroalkyl substances (PFAS) and latent health outcomes: A review including the placenta as a target tissue and possible driver of peri- and postnatal effects', *Toxicology*, 443, p. 152565. Available at: https://doi.org/10.1016/j.tox.2020.152565.

Bolisetty, S., Peydayesh, M. and Mezzenga, R. (2019) 'Sustainable technologies for water purification from heavy metals: review and analysis', *Chemical Society Reviews*, 48(2), pp. 463–487. Available at: https://doi.org/10.1039/C8CS00493E.

Boonya-atichart, A., Boontanon, S.K. and Boontanon, N. (2018) 'Study of hybrid membrane filtration and photocatalysis for removal of perfluorooctanoic acid (PFOA) in groundwater', *Water Science and Technology*, 2017(2), pp. 561–569. Available at: https://doi.org/10.2166/wst.2018.178.

Couto, C.F. *et al.* (2020) 'Assessing potential of nanofiltration, reverse osmosis and membrane distillation drinking water treatment for pharmaceutically active compounds (PhACs) removal', *Journal of Water Process Engineering*, 33, p. 101029. Available at: https://doi.org/10.1016/j.jwpe.2019.101029.

Crone, B.C. *et al.* (2019) 'Occurrence of per- and polyfluoroalkyl substances (PFAS) in source water and their treatment in drinking water', *Critical Reviews in Environmental Science and Technology*, 49(24), pp. 2359–2396. Available at: https://doi.org/10.1080/10643389.2019.1614848.

Cserbik, D. *et al.* (2023) 'Human exposure to per- and polyfluoroalkyl substances and other emerging contaminants in drinking water', 6, p. 16. Available at: https://doi.org/10.1038/s41545-023-00236-y.

Dagher, G. *et al.* (2023) 'Understanding and predicting the adsorption and rejection of pesticides and metabolites by hollow fiber nanofiltration membranes', *Separation and Purification Technology*, 330, p. 125323. Available at: https://doi.org/10.1016/j.seppur.2023.125323.

Das, S. and Ronen, A. (2022) 'A Review on Removal and Destruction of Per- and Polyfluoroalkyl Substances (PFAS) by Novel Membranes', *Membranes*, 12(7), p. 662. Available at: https://doi.org/10.3390/membranes12070662.

Domingo, J.L. and Nadal, M. (2019) 'Human exposure to per- and polyfluoroalkyl substances (PFAS) through drinking water: A review of the recent scientific literature', *Environmental Research*, 177, p. 108648. Available at: https://doi.org/10.1016/j.envres.2019.108648.

Flores, C. *et al.* (2013) 'Occurrence of perfluorooctane sulfonate (PFOS) and perfluorooctanoate (PFOA) in N.E. Spanish surface waters and their removal in a drinking water treatment plant that combines conventional and advanced treatments in parallel lines', *Science of The Total Environment*, 461–462, pp. 618–626. Available at: https://doi.org/10.1016/j.scitotenv.2013.05.026.

Furlow, B. (2024) 'US EPA sets historic new restrictions on toxic PFAS in drinking water', *The Lancet Oncology*, 25(5), p. e181. Available at: https://doi.org/10.1016/S1470-2045(24)00215-8.

Giglioli, S., Colombo, L. and Azzellino, A. (2023) 'Cluster and multivariate analysis to study the diffuse contamination of emerging per- and polyfluoroalkyl substances (PFAS) in the Veneto Region plain (North-eastern Italy)', *Chemosphere*, 319, p. 137916. Available at: https://doi.org/10.1016/j.chemosphere.2023.137916.

Glüge, J. *et al.* (2020) 'An overview of the uses of per- and polyfluoroalkyl substances (PFAS)', *Environmental Science: Processes & Impacts*, 22(12), pp. 2345–2373. Available at: https://doi.org/10.1039/D0EM00291G.

Gobelius, L. *et al.* (2018) 'Per- and Polyfluoroalkyl Substances in Swedish Groundwater and Surface Water: Implications for Environmental Quality Standards and Drinking Water Guidelines', *Environmental Science & Technology*, 52(7), pp. 4340–4349. Available at: https://doi.org/10.1021/acs.est.7b05718.

Hammes, F. *et al.* (2011) '6.41 - Biotreatment of Drinking Water', in M. Moo-Young (ed.) *Comprehensive Biotechnology (Second Edition)*. Burlington: Academic Press, pp. 517–530. Available at: https://doi.org/10.1016/B978-0-08-088504-9.00386-X.

Hang, X. *et al.* (2015) 'Removal and recovery of perfluorooctanoate from wastewater by nanofiltration', *Separation and Purification Technology*, 145, pp. 120–129. Available at: https://doi.org/10.1016/j.seppur.2015.03.013.

Hara-Yamamura, H. *et al.* (2022) 'Rejection of perfluorooctanoic acid (PFOA) and perfluorooctane sulfonate (PFOS) by severely chlorine damaged RO membranes with different salt rejection ratios', *Chemical Engineering Journal*, 446, p. 137398. Available at: https://doi.org/10.1016/j.cej.2022.137398.

Harrad, S. *et al.* (2019) 'Perfluoroalkyl Substances in Drinking Water, Indoor Air and Dust from Ireland: Implications for Human Exposure', *Environmental Science & Technology*, 53(22), pp. 13449–13457. Available at: https://doi.org/10.1021/acs.est.9b04604.

'Health and Environment Alliance | How PFAS pollution affects people's health across Europe' (2018) *Health and Environment Alliance*. Available at: https://www.env-health.org/banpfas/ (Accessed: 30 May 2024).

*Health and environmental impacts prompt a call for strict ruling on ubiquitous 'forever chemicals'* (2023). Available at: https://environment.ec.europa.eu/news/health-and-environmental-impacts-prompt-call-strict-ruling-ubiquitous-forever-chemicals-2023-10-19_en (Accessed: 30 May 2024).

Hopkins, Z.R. *et al.* (2018) 'Recently Detected Drinking Water Contaminants: GenX and Other Per- and Polyfluoroalkyl Ether Acids', *Journal AWWA*, 110(7), pp. 13–28. Available at: https://doi.org/10.1002/awwa.1073.

Ingold, V., Kämpfe, A. and Ruhl, A.S. (2023) 'Screening for 26 per- and polyfluoroalkyl substances (PFAS) in German drinking waters with support of residents', *Eco-Environment & Health*, 2(4), pp. 235–242. Available at: https://doi.org/10.1016/j.eehl.2023.08.004.

Jiang, L. *et al.* (2021) 'Comprehensive multi-omics approaches reveal the hepatotoxic mechanism of perfluorohexanoic acid (PFHxA) in mice', *Science of The Total Environment*, 790, p. 148160. Available at: https://doi.org/10.1016/j.scitotenv.2021.148160.

Jin, T. *et al.* (2021) 'Amyloid fibril-based membranes for PFAS removal from water', *Environmental Science: Water Research & Technology*, 7(10), pp. 1873–1884. Available at: https://doi.org/10.1039/D1EW00373A.

Jin, T., Peydayesh, M. and Mezzenga, R. (2021) 'Membrane-based technologies for per- and poly-fluoroalkyl substances (PFASs) removal from water: Removal mechanisms, applications, challenges and perspectives', *Environment International*, 157, p. 106876. Available at: https://doi.org/10.1016/j.envint.2021.106876.

Johnson, J.K. *et al.* (2019) 'Advanced Filtration Membranes for the Removal of Perfluoroalkyl Species from Water', *ACS Omega*, 4(5), pp. 8001–8006. Available at: https://doi.org/10.1021/acsomega.9b00314.

Kärrman, A. *et al.* (2019) *PFASs in the Nordic environment*. 2019:515. Copenhagen: Nordic Council of Ministers (TemaNord). Available at: https://doi.org/10.6027/TN2019-515.

*Keeping our water clean: the case of water contamination in the Veneto Region, Italy* (2017). Available at: https://iris.who.int/handle/10665/344113 (Accessed: 31 May 2024).

Kim, K.Y. *et al.* (2020) 'Perfluoroalkyl substances and pharmaceuticals removal in full-scale drinking water treatment plants', *Journal of Hazardous Materials*, 400, p. 123235. Available at: https://doi.org/10.1016/j.jhazmat.2020.123235.

Kumar, R. *et al.* (2023) 'Microbial and thermal treatment techniques for degradation of PFAS in bio-solids: A focus on degradation mechanisms and pathways', *Journal of Hazardous Materials*, 452, p. 131212. Available at: https://doi.org/10.1016/j.jhazmat.2023.131212.

Kurwadkar, S. *et al.* (2022) 'Per- and polyfluoroalkyl substances in water and wastewater: A critical review of their global occurrence and distribution', *The Science of the total environment*, 809, p. 151003. Available at: https://doi.org/10.1016/j.scitotenv.2021.151003.

Lee, T., Speth, T.F. and Nadagouda, M.N. (2022) 'High-pressure membrane filtration processes for separation of Per- and polyfluoroalkyl substances (PFAS)', *Chemical Engineering Journal*, 431, p. 134023. Available at: https://doi.org/10.1016/j.cej.2021.134023.

Li, N. *et al.* (2021) 'Perfluoroalkyl substances in the urine and hair of preschool children, airborne particles in kindergartens, and drinking water in Hong Kong', *Environmental Pollution*, 270, p. 116219. Available at: https://doi.org/10.1016/j.envpol.2020.116219.

Liu, C. *et al.* (2022) 'Evaluating the efficiency of nanofiltration and reverse osmosis membrane processes for the removal of per- and polyfluoroalkyl substances from water: A critical review', *Separation and Purification Technology*, 302, p. 122161. Available at: https://doi.org/10.1016/j.seppur.2022.122161.

Liu, C.J. *et al.* (2021) 'Pilot-scale field demonstration of a hybrid nanofiltration and UV-sulfite treatment train for groundwater contaminated by per- and polyfluoroalkyl substances (PFASs)', *Water Research*, 205, p. 117677. Available at: https://doi.org/10.1016/j.watres.2021.117677.

Liu, C.J., Strathmann, T.J. and Bellona, C. (2021) 'Rejection of per- and polyfluoroalkyl substances (PFASs) in aqueous film-forming foam by high-pressure membranes', *Water Research*, 188, p. 116546. Available at: https://doi.org/10.1016/j.watres.2020.116546.

Liu, L. *et al.* (2021) 'Dynamics of freezing/thawing indices and frozen ground from 1900 to 2017 in the upper Brahmaputra River Basin, Tibetan Plateau', *Advances in Climate Change Research*, 12(1), pp. 6–17.

Livsmedelsverkets föreskrifter om dricksvatten. SLVFS 2001:30

Ma, Q. *et al.* (2024) 'Evaluation of commercial nanofiltration and reverse osmosis membrane filtration to remove per-and polyfluoroalkyl substances (PFAS): Effects of transmembrane pressures and water matrices', *Water Environment Research: A Research Publication of the Water Environment Federation*, 96(2), p. e10983. Available at: https://doi.org/10.1002/wer.10983.

Mahlangu, O.T. *et al.* (2023) 'Fouling of high pressure-driven NF and RO membranes in desalination processes: Mechanisms and implications on salt rejection', *Chemical Engineering Research and Design*, 199, pp. 268–295. Available at: https://doi.org/10.1016/j.cherd.2023.09.037.

Manea, S. *et al.* (2020) 'Exposure to PFAS and small for gestational age new-borns: A birth records study in Veneto Region (Italy)', *Environmental Research*, 184, p. 109282. Available at: https://doi.org/10.1016/j.envres.2020.109282.

Mastropietro, T.F. *et al.* (2021) 'Reverse osmosis and nanofiltration membranes for highly efficient PFASs removal: overview, challenges and future perspectives', *Dalton Transactions*, 50(16), pp. 5398–5410. Available at: https://doi.org/10.1039/D1DT00360G.

Metcalfe, C.D. *et al.* (2022) 'An introduction to the sources, fate, occurrence and effects of endocrine disrupting chemicals released into the environment', *Environmental Research*, 207, p. 112658. Available at: https://doi.org/10.1016/j.envres.2021.112658.

Mirbagheri, S.A. *et al.* (2016) 'Removing Fe, Zn and Mn from steel making plant wastewater using RO and NF membranes', *Iranian Journal of Health Sciences*, 4, pp. 41–55. Available at: https://doi.org/10.18869/acadpub.jhs.4.4.41.

Mojiri, A. *et al.* (2023) 'Occurrence of per- and polyfluoroalkyl substances in aquatic environments and their removal by advanced oxidation processes', *Chemosphere*, 330, p. 138666. Available at: https://doi.org/10.1016/j.chemosphere.2023.138666.

Müller, M.H.B. *et al.* (2019) 'Prenatal exposure to persistent organic pollutants in Northern Tanzania and their distribution between breast milk, maternal blood, placenta and cord blood', *Environmental Research*, 170, pp. 433–442. Available at: https://doi.org/10.1016/j.envres.2018.12.026.

*New limit values for PFAS in drinking water in Sweden - LIFE SOuRCE* (2023). Available at: https://life-source.se/nyheter_sv/new-limit-values-for-pfas-in-drinking-water-in-sweden/ (Accessed: 31 May 2024).

*Synthesis paper on per- and polyfluorinated chemicals (PFCs)* (2013)*. OECD Environment, Health and Safety Publications.* Available at: https://www.oecd.org/env/ehs/risk-management/PFC_FINAL-Web.pdf

Park, H. *et al.* (2018) 'Evaluation of the current contamination status of PFASs and OPFRs in South Korean tap water associated with its origin', *Science of The Total Environment*, 634, pp. 1505–1512. Available at: https://doi.org/10.1016/j.scitotenv.2018.04.068.

*Perfluoroalkyl and Polyfluoroalkyl Substances (PFAS)* (2023) *National Institute of Environmental Health Sciences*. Available at: https://www.niehs.nih.gov/health/topics/agents/pfc (Accessed: 31 May 2024).

Peritore, A.F. *et al.* (2023) 'Current Review of Increasing Animal Health Threat of Per- and Polyfluoro-alkyl Substances (PFAS): Harms, Limitations, and Alternatives to Manage Their Toxicity', *International Journal of Molecular Sciences*, 24(14), p. 11707. Available at: https://doi.org/10.3390/ijms241411707.

Petersen, R.J. (1993) 'Composite reverse osmosis and nanofiltration membranes', *Journal of Membrane Science*, 83(1), pp. 81–150. Available at: https://doi.org/10.1016/0376-7388(93)80014-O.

*PFAS - Kemikalieinspektionen* (2023). Available at: https://www.kemi.se/en/chemical-substances-and-materials/pfas (Accessed: 31 May 2024).

*PFAS - the poison on everyone's lips* (2022) *Vattenbokhandeln*. Available at: https://vattenbokhandeln.svensktvatten.se/produkt/pfas-the-poison-on-everyones-lips/ (Accessed: 31 May 2024).

*PFAS in tap water | ZeroWater Europe* (2022). Available at: https://www.zerowater.eu/pfas-in-tap-water/ (Accessed: 31 May 2024).

*PFAS Water Contamination Scandals Unfold Across Europe* (2023) *CHEM Trust*. Available at: https://chemtrust.org/news/pfas-pollution-scandals/ (Accessed: 30 May 2024).

Pilli, S. *et al.* (2021) 'Detection and removal of poly and perfluoroalkyl polluting substances for sustainable environment', *Journal of Environmental Management*, 297, p. 113336. Available at: https://doi.org/10.1016/j.jenvman.2021.113336.

Qiao, X. *et al.* (2020) 'Contamination profiles and risk assessment of per- and polyfluoroalkyl substances in groundwater in China', *Environmental Monitoring and Assessment*, 192(2), p. 76. Available at: https://doi.org/10.1007/s10661-019-8005-z.

*Ringsjöverket* (2015) *Sydvatten*. Available at: https://sydvatten.se/var-verksamhet/vattenverk/ringsjoverket/ (Accessed: 31 May 2024).

*RSC challenges UK Government to reduce PFAS levels in British water as research highlights serious health risks posed by 'forever chemicals'* (2024). Available at: https://www.rsc.org/news-events/articles/2023/oct/pfas-cleaning-up-uk-drinking-water/ (Accessed: 31 May 2024).

Safulko, A. *et al.* (2023) 'Rejection of perfluoroalkyl acids by nanofiltration and reverse osmosis in a high-recovery closed-circuit membrane filtration system', *Separation and Purification Technology*, 326, p. 124867. Available at: https://doi.org/10.1016/j.seppur.2023.124867.

Shivakoti, B. *et al.* (2010) 'Perfluorinated chemicals (PFCs) in water purification plants (WPPs) with advanced treatment processes', *Water Science & Technology: Water Supply*, 10. Available at: https://doi.org/10.2166/ws.2010.707.

Skaggs, C.S. and Logue, B.A. (2021) 'Ultratrace analysis of per- and polyfluoroalkyl substances in drinking water using ice concentration linked with extractive stirrer and high performance liquid chromatography – tandem mass spectrometry', *Journal of Chromatography A*, 1659, p. 462493. Available at: https://doi.org/10.1016/j.chroma.2021.462493.

Sörengård, M. *et al.* (2022) 'Long-distance transport of per- and polyfluoroalkyl substances (PFAS) in a Swedish drinking water aquifer', *Environmental Pollution*, 311, p. 119981. Available at: https://doi.org/10.1016/j.envpol.2022.119981.

Soriano, Á., Gorri, D. and Urtiaga, A. (2019) 'Selection of High Flux Membrane for the Effective Removal of Short-Chain Perfluorocarboxylic Acids', *Industrial & Engineering Chemistry Research*, 58(8), pp. 3329–3338. Available at: https://doi.org/10.1021/acs.iecr.8b05506.

Soriano, A., Schaefer, C. and Urtiaga, A. (2020) 'Enhanced treatment of perfluoroalkyl acids in groundwater by membrane separation and electrochemical oxidation', *Chemical Engineering Journal Advances*, 4, p. 100042. Available at: https://doi.org/10.1016/j.ceja.2020.100042.

Southerland, E. and Birnbaum, L.S. (2023) 'What Limits Will the World Health Organization Recommend for PFOA and PFOS in Drinking Water?', *Environmental Science & Technology*, 57(18), pp. 7103–7105. Available at: https://doi.org/10.1021/acs.est.3c02260.

Steinle-Darling, E. and Reinhard, M. (2008) 'Nanofiltration for Trace Organic Contaminant Removal: Structure, Solution, and Membrane Fouling Effects on the Rejection of Perfluorochemicals', *Environmental Science & Technology*, 42(14), pp. 5292–5297. Available at: https://doi.org/10.1021/es703207s.

Stoiber, T. *et al.* (2020) 'PFAS in drinking water: an emergent water quality threat'.

Tang, C.Y. *et al.* (2006) 'Use of Reverse osmosis Membranes to Remove Perfluorooctane Sulfonate (PFOS) from Semiconductor Wastewater', *Environmental Science & Technology*, 40(23), pp. 7343–7349. Available at: https://doi.org/10.1021/es060831q.

Tang, C.Y. *et al.* (2007) 'Effect of Flux (Transmembrane Pressure) and Membrane Properties on Fouling and Rejection of Reverse osmosis and Nanofiltration Membranes Treating Perfluorooctane Sulfonate Containing Wastewater', *Environmental Science & Technology*, 41(6), pp. 2008–2014. Available at: https://doi.org/10.1021/es062052f.

Thompson, J., Eaglesham, G. and Mueller, J. (2011) 'Concentrations of PFOS, PFOA and other perfluorinated alkyl acids in Australian drinking water', *Chemosphere*, 83(10), pp. 1320–1325. Available at: https://doi.org/10.1016/j.chemosphere.2011.04.017.

Tokranov, A.K. *et al.* (2021) 'Surface-water/groundwater boundaries affect seasonal PFAS concentrations and PFAA precursor transformations', *Environmental Science: Processes & Impacts*, 23(12), pp. 1893–1905. Available at: https://doi.org/10.1039/D1EM00329A.

*Treatment of drinking water to remove PFAS (Signal) | European zero pollution dashboards* (2024). Available at: https://www.eea.europa.eu/en/european-zero-pollution-dashboards/indicators/treatment-of-drinking-water-to-remove-pfas-signal (Accessed: 31 May 2024).

Urtiaga, A. (2021) 'Electrochemical technologies combined with membrane filtration', *Current Opinion in Electrochemistry*, 27, p. 100691. Available at: https://doi.org/10.1016/j.coelec.2021.100691.

*Vombverket* (2015) *Sydvatten*. Available at: https://sydvatten.se/var-verksamhet/vattenverk/vombverket/ (Accessed: 31 May 2024).

Wang, J. *et al.* (2018) 'Perfluorooctane sulfonate and perfluorobutane sulfonate removal from water by nanofiltration membrane: The roles of solute concentration, ionic strength, and macromolecular organic foulants', *Chemical Engineering Journal*, 332, pp. 787–797. Available at: https://doi.org/10.1016/j.cej.2017.09.061.

*WHO/EU drinking water standards comparative table* (2024). Available at: https://www.lenntech.com/who-eu-water-standards.htm (Accessed: 30 May 2024).

Woldegiorgis, A. *et al.* (2005) 'Results from the Swedish National Screening Programme 2005. Sub-report 3: Perfluorinated Alkylated Substances (PFAS)'.

Yan, H. *et al.* (2015) 'Occurrence of perfluorinated alkyl substances in sediment from estuarine and coastal areas of the East China Sea', *Environmental Science and Pollution Research*, 22(3), pp. 1662–1669. Available at: https://doi.org/10.1007/s11356-014-2838-3.

Zhao, C. *et al.* (2013) 'Perfluorooctane sulfonate removal by nanofiltration membrane the role of calcium ions', *Chemical Engineering Journal*, 233, pp. 224–232. Available at: https://doi.org/10.1016/j.cej.2013.08.027.

Zhi, Y. *et al.* (2022) 'Removing emerging perfluoroalkyl ether acids and fluorotelomer sulfonates from water by nanofiltration membranes: Insights into performance and underlying mechanisms', *Separation and Purification Technology*, 298, p. 121648. Available at: https://doi.org/10.1016/j.seppur.2022.121648.

# Appendix

## PFAS concentration calculation

Calculation step (Prepare water samples)

PFAS standard mixture (FX19) has a concentration of each PFAS in the sample = **0.10 mg/mL**

We will take a spike amount = **0.08955 mL**

- **$C = m/V$**

C = Concentration,

m = mass of solute dissolved

V = Volume of solution

- m (absolute) = 0.10 mg/mL * 0.08955 mL = 0.008955 mg = **8.955 μg PFAS**

**0.08955 mL** of the Spike solution which contains 8.955 µg of PFAS will then be mixed with **(7.5 L + dead vol = 1.255 + 0.2 L) = 8.955 L** of drinking water into the feed tank.

Total volume of water = **8955 mL**

- Concentration of PFAS in the drinking water sample solution

  **= 8.955 μg/8955 mL = 0.001 μg/mL = 1 μg/L**

# Sample bottle naming

Table A. For water quality analysis with NF membranes

| Serial No. | Sample type (NF) | Bottle Name (NF) |
|---|---|---|
| 1 | Blank (Clean drinking water) from the tap at the beginning of the experiment (200 mL) | Blank (NF) |
| 2 | Reference (Drinking water + spike solution) from the feed tank at the beginning of the experiment (200 mL) | Reference (NF) |
| 3 | Feed at the beginning (at stable flux) (200 mL) | Feed S (NF) |
| 4 | Permeate 1 (FilmTec NF90) at the beginning at a stable flux (200 mL) | NF90 S |
| 5 | Permeate 2 (FilmTec NF270) at the beginning at a stable flux (200 mL) | NF270 S |
| 6 | Permeate 3 (Alfa Laval NF99HF) at the beginning at a stable flux (200 mL) | NF99HF S |
| 7 | Permeate 4 (Alfa Laval NF) at the beginning at a stable flux (200 mL) | NF S |
| 8 | Feed at the end (around 50% recovery) (200 mL) | Feed E (NF) |
| 9 | Permeate 1 (FilmTec NF90) at the end (200 mL) | NF90 E |
| 10 | Permeate 2 (FilmTec NF270) at the beginning at a stable flux (200 mL) | NF270 E |
| 11 | Permeate 3 (Alfa Laval NF99HF) at the end (200 mL) | NF99HF E |
| 12 | Permeate 4 (Alfa Laval NF) at the end (200 mL) | NF E |

Table B. For water quality analysis with RO membranes

| Serial No. | Sample type (RO) | Bottle Name (RO) |
|---|---|---|
| 1 | Blank (Clean drinking water) from the tap at the beginning of the experiment (200 mL) | Blank (RO) |
| 2 | Reference (Drinking water + spike solution) from the feed tank at the beginning of the experiment (200 mL) | Reference (RO) |
| 3 | Feed at the beginning (at stable flux) (200 mL) | Feed S (RO) |
| 4 | Permeate 1 (FilmTec BW30) at the beginning at a stable flux (200 mL) | BW30 S |
| 5 | Permeate 2 (Alfa Laval RO99) at the beginning at a stable flux (200 mL) | RO99 S |
| 6 | Permeate 3 (Alfa Laval RO98 pHt$^{TM}$) at the beginning at a stable flux (200 mL) | RO98 pHt$^{TM}$ S |
| 7 | Permeate 4 (Alfa Laval RO90) at the beginning at a stable flux (200 mL) | RO90 S |
| 8 | Feed at the end (around 50% recovery) (200 mL) | Feed E (RO) |
| 9 | Permeate 1 (FilmTec BW30) at the end (200 mL) | BW30 E |
| 10 | Permeate 2 (Alfa Laval RO99) at the beginning at a stable flux (200 mL) | RO99 E |
| 11 | Permeate 3 (Alfa Laval RO98 pHt$^{TM}$) at the end (200 mL) | RO98 pHt$^{TM}$ E |
| 12 | Permeate 4 (Alfa Laval RO90) at the end (200 mL) | RO90 E |